New Astronomy Reviews 91 (2020) 101547

Contents lists available at ScienceDirect

New Astronomy Reviews

journal homepage: www.elsevier.com/locate/newastrev

INTEGRAL View on cataclysmic variables and symbiotic binaries

Alexander Lutovinov[*,a,b], Valery Suleimanov[c,d,e], Gerardo Juan Manuel Luna[f,g,h], Sergey Sazonov[i,j], Domitilla de Martino[k], Lorenzo Ducci[l,m], Victor Doroshenko[n,o], Maurizio Falanga[p]

[a] Space Research Institute, Profsoyuznaya str. 84/32, 117997 Moscow, Russia
[b] Moscow Institute of Physics and Technology, Dolgoprudny, Moscow Region, 141700, Russia
[c] Institute for Astronomy and Astrophysics, University of Tübingen, Sand 1, 72026 Tübingen, Germany
[d] Space Research Institute, Profsoyuznaya str. 84/32, 117997 Moscow, Russia
[e] Kazan Federal University, Kremlevskaya 18, 420008 Kazan, Russia
[f] CONICET-Universidad de Buenos Aires, Instituto de Astronoma y Fsica del Espacio (IAFE), Av. Inte. Güiraldes 2620, C1428ZAA, Buenos Aires, Argentina
[g] Universidad de Buenos Aires, Facultad de Ciencias Exactas y Naturales, Buenos Aires, Argentina
[h] Universidad Nacional de Hurlingham, Av. Gdor. Vergara 2222, Villa Tesei, Buenos Aires, Argentina
[i] Space Research Institute, Profsoyuznaya str. 84/32, 117997 Moscow, Russia
[j] Moscow Institute of Physics and Technology, Dolgoprudny, Moscow Region, 141700, Russia
[k] INAF - Capodimonte Astronomical Observatory Naples Via Moiariello 16, I-80131 Naples, Italy
[l] Institute for Astronomy and Astrophysics, University of Tübingen, Sand 1, 72026 Tübingen, Germany
[m] ISDC Data Center for Astrophysics, Université de Genève, 16 chemin d'Écogia, 1290 Versoix, Switzerland
[n] Institute for Astronomy and Astrophysics, University of Tübingen, Sand 1, 72026 Tübingen, Germany
[o] Space Research Institute, Profsoyuznaya str. 84/32, 117997 Moscow, Russia
[p] International Space Science Institute, Hallerstrasse 6, CH-3012 Bern, Switzerland

ARTICLE INFO

Keywords:
Cataclysmic variables
Symbiotic stars
X-Ray
White dwarfs

ABSTRACT

Accreting white dwarfs (WDs) constitute a significant fraction of the hard X-ray sources detected by the *INTEGRAL* observatory. Most of them are magnetic Cataclysmic Variables (CVs) of the intermediate polar (IP) and polar types, but the contribution of the Nova-likes systems and the systems with optically thin boundary layers, Dwarf Novae (DNs) and Symbiotic Binaries (or Symbiotic Stars, SySs) in quiescence is also not negligible. Here we present a short review of the results obtained from the observations of cataclysmic variables and symbiotic binaries by *INTEGRAL*. The highlight results include the significant increase of the known IP population, determination of the WD mass for a significant fraction of IPs, the establishment of the luminosity function of magnetic CVs, and uncovering origin of the Galactic ridge X-ray emission which appears to largely be associated with hard emission from magnetic CVs.

1. Introduction

Cataclysmic variables (CVs) is a broad class of close binary systems with an accreting white dwarf (WD) as a primary (see a detailed review in the book by Warner (2003)). The virial temperature of protons at the WD surface is about a few tens of keV, so the optically thin accretion flow shocked above the WD surface, inevitably produces an optically thin free-free radiation with the comparable temperatures. Therefore, a significant fraction of CVs appear as hard X-ray sources.

The first model describing this process in the case of the spherical accretion on the WD surface was proposed by Aizu (1973). Soon it was recognized that this model is oversimplified and far from the reality. The local shock areas near magnetic poles, which are shaped by the strong magnetic field of the WD, were proposed as the most likely origin of the observed hard X-ray radiation in CVs (see, e.g. Fabian et al., 1976). Almost at the same time it was found that the well known CV AM Her was detected with the *Uhuru* observatory as an X-ray source (3U 1809 + 50) Giacconi et al. (1974). The source also showed a significant optical polarization (Tapia, 1977), indicating the presence of a strongly magnetized WD in the system, and thus supported the hypothesis that the observed hard X-ray emission was originating in the hot plasma heated by the shock above the WD surface. For this particular object (AM Her) the spin period is equal to the orbital period, therefore all similar CVs are named synchronous polars (from the

* Corresponding author.
E-mail address: aal@iki.rssi.ru (A. Lutovinov).

https://doi.org/10.1016/j.newar.2020.101547
Received 25 November 2019; Received in revised form 12 September 2020; Accepted 18 September 2020
Available online 23 November 2020

polarized optical emission) or AM Her type stars. There is no accretion disc in such systems and the magnetic field strength of the WD ($10^7 - 10^8$ G) is sufficient to synchronize the spin period with the orbital one. Note that the synchronization is possible only for relatively compact systems, so most polars have relatively short orbital periods < 5 h (see, e.g., Norton et al. (2004)).

The first objects belonging to another type of magnetic CVs, the intermediate polars (IPs), were discovered as X-ray sources in the late of 70th (TV Col Charles et al. (1979) and AO Psc Griffiths et al., 1980). Spin periods of WDs in such systems are much shorter compared to orbital ones, and most of them did not display any optical polarization (see, e.g., Ferrario et al., 2015). Unlike polars, in IPs systems there was clear evidence for presence of an accretion disc (see details in Warner (2003)). The magnetic field strength in these systems is believed to be lower than in polars ($< 1 - 3 \times 10^6$ G), thus allowing the formation of an accretion disc. It is also not strong enough to synchronize the WD rotation with the orbital period. As a consequence, the accretion disk is truncated at some radius defined as the magnetospheric radius, $R_{\rm m}$, where the magnetic and accretion pressures balance. Surprisingly, this subclass of the magnetic CVs has been found to be the most numerous among the hard X-ray emitting CVs discovered by *INTEGRAL*.

A crucial parameter of magnetic CVs, which can be learned from hard X-ray observations, is a mass of the WD. Indeed, the temperature below the shock is defined by a compactness of the WD, i.e., by the ratio of its mass and radius. On the other hand, the relation between mass and radius of the WD is well established (see, e.g. Nauenberg, 1972). Therefore, it is possible to estimate the WD mass based on the observed plasma temperature, which in turn can be derived from the approximation of its hard X-ray spectrum with an optically thin emission as the bremsstrahlung model (see, e.g., Rothschild et al., 1981 for the first results). Later more detailed models of the so-called post-shock region (PSR) where the observed emission is produced were developed (Canalle et al., 2005; Cropper et al., 1999; Saxton et al., 2007; Woelk and Beuermann, 1996; Wu et al., 1994) and used to estimate the WD masses in magnetic CVs (see, e.g., Cropper et al., 1998; Ramsay, 2000).

Note, that these early works used a relatively soft ($E < 20$ keV) part of IP X-ray spectra measured with the *Ginga* observatory and *RXTE*/PCA instrument. Later, the same approach was applied to observations in hard X-rays with the *RXTE*/HEXTE, *Swift*/BAT instruments and with the *Suzaku* observatory (see, e.g., Brunschweiger et al., 2009; Suleimanov et al., 2005; Yuasa et al., 2010). A number of articles was dedicated to measure the masses of individual IPs or smaller samples of objects (see, e.g., Anzolin et al., 2009; Bernardini et al., 2012, 2013, 2015, 2018, 2019). Recently, the high sensitivity of the *NuSTAR* observatory in hard X-rays has been exploited for the same purposes (see, e.g., Shaw et al., 2018; Suleimanov et al., 2019; Wada et al., 2018). The *INTEGRAL* observatory (Winkler et al., 2003) played also an important role in the investigations of CVs. In particular, hard X-ray spectra in many IP systems obtained by the IBIS telescope were used to determine WD masses, starting from the early papers (Falanga et al., 2005; Revnivtsev et al., 2004).

Obviously, the determination of parameters of individual IPs is possible only for relatively close, bright sources. At the same time an extended hard X-ray emission, registered from the Galactic Center and Galactic ridge, can be explained as collective emission of a large number of unresolved CVs. This hypothesis, initially proposed by Revnivtsev et al. (2006b), was later confirmed in number of papers (Hailey et al., 2016; Revnivtsev et al., 2008; Sazonov et al., 2006). Thus, the study of the Galactic ridge emission is tightly connected with the analysis of individual CVs properties, and the *INTEGRAL* observatory contributed significantly in this area.

It is important to note that the magnetic CVs are not the only WDs capable of producing hard X-ray emission (see e.g. Mukai, 2017). For instance, hard X-ray emission from Dwarf Novae (DN) was already discovered at the end of 70s (see, e.g. Heise et al., 1978; Swank et al., 1978) during their quiescent states. These results were interpreted as radiation of the optically thin boundary layer between the WD surface and the accretion disc feeding the WD at low mass accretion rates (Pringle and Savonije, 1979; Tylenda, 1981). The system SS Cyg is the best characterized DN in hard X-rays at the present time (see, e.g. Balman and Revnivtsev, 2012; McGowan et al., 2004). In addition to DNs, Novalike systems have been detected in the hard X-rays although some of them are disputed to be magnetic (e.g. IGR J12123-5802 (Bernardini et al., 2013); TW Pic (Norton et al., 2000)).

Symbiotic Stars (SySs) are a quite small subclass of binary systems, which emit in X-rays due to the accretion onto compact objects. The donor star in such systems is a red giant, and it gives a main contribution in the optical luminosity. A compact object (typically a WD, but there are several systems with neutron stars) accretes the matter from donor wind producing ultraviolet and X-ray emission extending down to the blue optical spectral band (see recent review (Munari, 2019) and references therein). Below we will focus on the systems with WDs as an accretor. The SySs with neutron stars are characterised in a separate review paper in this volume.

The first SySs with accreting WDs were discovered by the *Einstein* observatory at the beginning of the 80s (Allen, 1981; Anderson et al., 1981; Cordova et al., 1981). The origin of the X-ray radiation in such systems can be similar to that in CVs although they show also some remarkable difference with respect to them. In particular, there are super-soft sources with permanent thermonuclear burning on the WD surface, like the AG Dra system. Boundary layers between accretion disks and WDs are considered as most probable sources of X-ray radiation in less luminous systems. The hard X-ray emission of RT Cru discovered by *INTEGRAL* (Chernyakova et al., 2005) was proposed to originate from an optically thin boundary layer.

Here we present a detailed review of the results concerning various types of CVs, obtained with the *INTEGRAL* observatory. The review includes theoretical explanations discussed in connection with properties of individual sources and their populations such as the luminosity function and contribution to the Galactic ridge emission.

2. CVs and SySs observed by *INTEGRAL*

A significant part of the *INTEGRAL* observational program is dedicated to surveys of different regions of the Galactic plane and its regular scans with the purpose to map the Galaxy, detect new sources and to study in details all detected objects. The main instrument of the observatory for such investigations is the ISGRI detector of the IBIS telescope, ISGRI/IBIS (the Imager on Board the INTEGRAL Satellite / INTEGRAL Soft Gamma Ray Imager, Lebrun et al. (2003)). During more than 15 years *INTEGRAL* performed the deepest hard X-ray survey of the Galactic plane, which resulted in the discovery and characterization of many new and previously known sources which have been reported in many publications and particularly, the IBIS/ISGRI catalogues (see, e.g., Krivonos et al., 2012; Bird et al., 2016; Krivonos et al., 2017).

These surveys performed with *INTEGRAL*, besides producing general catalogues, have allowed to study different classes of sources, including the CVs. The first review of CVs, observed with *INTEGRAL*, was published by Barlow et al., 2006 and contained 19 known and newly discovered CVs. Most of them were IPs, but a couple of AM Her type systems and one dwarf Nova (SS Cyg) were also included. In a subsequent study, 22 objects were reported (Landi et al., 2009) and most of them were again IPs. In both works the hard X-ray spectra of the sources were fitted with bremsstrahlung and power-law models. For 11 sources the soft *Swift*/XRT spectra were also analysed in the follow-up work by Gehrels et al., 2004.

The Galactic plane surveys were extended further to the all-Sky surveys (see, e.g., Krivonos et al., 2012; Krivonos et al., 2017), which allowed to expand significantly the list of known hard X-ray sources. The current version of the general *INTEGRAL* source catalogue[1] contains a few tens of objects, identified as various types of CVs and

Symbiotic stars (see Table 1). We added some objects only recently identified as CVs, and marked as LMXB a source, which was erroneously identified earlier as CV de Martino et al. (2010).

In total, the table includes 78 objects: most of them are IPs and candidates (51 sources), seven sources are polars or AM Her type systems, six symbiotic stars, two dwarf Novae (SS Cyg and EI Psc), one pre-cataclysmic variable star (V1082 Sgr), one nova-like star (V347 Pup), and one possible double degenerate polar (IGR J05104-6910). It is possible that the last system is a close binary consisting of two WDs. There are also six candidate CVs which possibly are magnetic systems due to their hard X-ray radiation, and two candidate symbiotic stars. All references associated with the classification or re-classification of individual objects are presented in Table 1.

It is important to emphasize that a large fraction of CVs in the Table, namely 21, was either discovered or identified as such with the help of *INTEGRAL*. These sources are marked with asterisks. Note that some of them had already standard names for variable stars but were only identified as CVs by X-ray observations.

The identification of all hard X-ray sources started immediately after their discoveries by *INTEGRAL*, and it is obvious that new CVs were also a part of such programs (see, e.g., Masetti et al., 2006b; Bikmaev et al., 2006). Later significant efforts were made for the identifications of the unknown *INTEGRAL* X-ray sources, and new CVs were also revealed (Bernardini et al., 2012; Karasev et al., 2012; Lutovinov et al., 2012; Masetti et al., 2008, 2009, 2010, 2013; Rodriguez et al., 2009). Definitely, it is not possible to mention all papers devoted to identifications of the *INTEGRAL* sources, but the works which allowed to establish new CVs are listed in Table 1.

The signature feature of IPs are coherent X-ray pulsations with periods ranging from few hundreds to few thousands of seconds. The pulsations reflect the WD spin periods, and for IPs have to be significantly shorter than the orbital period. Therefore, if a candidate CV with a hard X-ray spectrum also displays coherent periodicities, it can be robustly confirmed as a magnetic CV. Most of the newly discovered CVs were identified as magnetic systems using the *XMM-Newton* observatory that allows long uninterrupted pointings and has high sensitivity in the soft 0.1-10 keV range (see e.g. de Martino et al., 2019 and references therein), however, *INTEGRAL* played important role in selection of the candidates. Other X-ray instruments such as *Swift*/XRT and *RXTE* also helped in establishing the CV nature of a number of *INTEGRAL* sources (see, e.g., Brunschweiger et al., 2009b; Butters et al., 2008; Butters et al., 2011; Suleimanov et al., 2019).

Another powerful method to identify CVs is optical spectroscopy. Optical spectra of such objects are characterised by blue continua with many emission lines, mainly corresponding to the Balmer series. Other typical emission features in optical spectra of magnetic CVs are the HeII (λ4686) line and the emission Bowen fluorescence blend (CIII/NIII spectral lines, seen mainly in the polars). The HeII emission arises from photoionization of material in the accretion disc and magnetically confined accretion flow by X-rays while the latter, the Bowen blend, originates in the irradiated face of the late-type companion star. The common criterion for IPs is an existence of a significant HeIIλ4686 emission line with the Equivalent Width (EW) of about 10Å. The ratio of EWs between the HeII and H_β lines provides a good discriminant for IPs, if $EW(HeII)/EW(H_\beta) > 0.5$ van Paradijs and Verbunt (1984). In turn, spectral identification of the optical counterpart as an evolved red giant star (spectral classes KIII - MIII) is a sufficient base to suggest that the given *INTEGRAL* source is a symbiotic star (see, e.g., Fortin et al., 2018; Masetti et al., 2008).

3. Models of hard X-ray emission sources in magnetic CVs

It is commonly accepted now that matter in-falling along the magnetic field lines forms a strong hydro-dynamical shock above the WD surface. The post-shock temperature is close to the virial one (Aizu, 1973; Fabian et al., 1976):

$$kT_{\rm sh} = \frac{3}{16}\mu m_{\rm H} V_{\rm ff}^2 \approx 32\, M_1 R_9^{-1}\ \ \text{keV}, \tag{1}$$

where $\mu \approx 0.62$ is the mean molecular weight of plasma with solar abundances, $m_{\rm H}$ is the proton mass, $V_{\rm ff}$ is the pre-shock free-fall velocity of the matter, M_1 is the WD mass in solar masses, and R_9 is the WD radius in units of 10^9 cm. Here we also assume that the kinetic energy of the ions converts equally efficient to the thermal energy of ions and electrons.

As it was mentioned above, the heated plasma in the PSR settles down as a subsonic flow on the WD surface and cools mainly due to a free-free and cyclotron emissions (Fabian et al., 1976; Lamb and Masters, 1979). The plasma velocity and its temperature are decreasing to values typical for the WD surface at the bottom of PSR. The height of the PSR is then determined by the cooling rate of the plasma. This implies that the settling time in the PSR has to be equal to the cooling time of the post-shock plasma. Such post-shock structures are sources of the observed X-ray emission in magnetized CVs.

The observed hard X-ray flux of the PSRs is, therefore, produced by free-free transitions in the hot post-shock plasma. The PSRs are optically thin for emerging free-free radiation, so hard X-ray spectra can be described as an optically thin thermal bremsstrahlung in the simpler case of a plasma with Hydrogen composition. The only free parameter in this case is the temperature, which appears to be an adequate estimate of the post-shock average temperature (see, however, next subsection). This opens the possibility to estimate the WD mass as the relation between WD mass and radius are well known (Nauenberg, 1972). This approach was first suggested and used by Rothschild et al. (Rothschild et al. (1981), see also Ishida (1991)). It is necessary to note that these estimates can only be correct for relatively weakly magnetized objects, i.e. the IPs. The magnetic field strengths at the WD surface in these objects are $< 1 - 3 \times 10^6$ G (Warner, 2003; Suleimanov et al., 2019), which provide the necessary condition for the free-free emission as a dominant cooling mechanism in PSRs in comparison with the cyclotron cooling (Lamb and Masters, 1979).

The total energy losses due to the cyclotron radiation depend both on the local plasma temperature and magnetic field strength. Therefore, they are most significant just after the shock, which leads to reduction of the maximum PSR temperature and, as a consequence, the observed bremsstrahlung temperature of the X-ray spectra. This is probably one of the reasons why not all polars are hard X-ray sources. However, it is important to note that the free-free cooling can dominate over the cyclotron cooling for luminous polars accreting at high rates, because of the high plasma density (Woelk and Beuermann, 1996). Therefore, such objects can be observed as hard X-ray sources.

Soon after the paper (Rothschild et al., 1981) it was recognized that a single bremsstrahlung spectrum is a rather crude approximation for the emergent spectra of PSRs. Done and Osborne (1997) suggested to use a number of spectra of optically thin plasma, since the optically thin plasma is multi-temperature. Therefore they used the cooling flow model with the emission measure power defined by the temperature distribution in the flow, i.e. $EM \sim (T/T_{\rm sh})^\alpha$. This approach is still used to model hard X-ray spectra of some intermediate polars (see, e.g. Wada et al., 2018). Fully hydro-dynamical PSR models (see below) can also be fitted to this relation (see Table 2 in for the comparison between different PSR models). Another possible approximation is to assume that the gas pressure is constant in the PSR (Frank et al., 2002). In this case $\alpha = 0.5$, and such a model was also used to study X-ray spectra of IPs (see e.g. Beardmore et al., 2000; Luna et al., 2015).

A more correct PSR model can be obtained using a self-consistent hydrodynamical description. Many works were devoted to this problem, and we can mention here just a few of them (Cropper et al., 1999; Woelk and Beuermann, 1996; Wu et al., 1994). The simplest model

[1] https://www.isdc.unige.ch/integral/catalog/latest/catalog.html

Table 1
List of CVs and SySs observed by *INTEGRAL*.

N	Source ID	Name	α_{2000}	δ_{2000}	Type	Ref
1	J002324.0+614132	V1033 Cas*	00:22:57.6	+61:41:08	IP	Bikmaev et al. (2006)
2	J002848.9+591722	V709 Cas	00:28:48.9	+59:17:22	IP	
3	J005524.0+461211	V515 And	00:55:24.0	+46:12:11	IP	Bikmaev et al. (2006)
4	J025604.1+192624	XY Ari	02:56:04.1	+19:26:24	IP	
5	J033111.8+435417	GK Per	03:31:11.8	+43:54:17	IP, DN, Nova	
6	J045707.4+452751	IGR J04571+4527*	04:57:07.0	+45:27:48	IP	Thorstensen and Halpern (2013)
7	J050227.5+244523	V1062 Tau	05:02:27.5	+24:45:23	IP	
8	J051029.3–691012	IGR J05104-6910*	05:10:29.3	-69:10:12	DDP?	Haberl et al. (2017)
9	J052522.5+241332	RX J0525.3+2413	05:25:22.7	+24:13:33	IP	Bernardini et al. (2015)
10	J052924.0–324840	TV Col	05:29:24.0	-32:48:40	IP	
11	J053450.5–580139	TW Pic	05:34:50.5	-58:01:39	IP?	
12	J054248.9+605132	BY Cam	05:42:48.9	+60:51:32	AM	
13	J055807.4+535443	V405 Aur	05:58:07.4	+53:54:43	IP	
14	J061033.6–484426	V347 Pup	06:10:33.6	-48:44:26	NL	Buckley et al. (1990)
15	J062516.1+733437	MU Cam	06:25:22.0	+73:36:07	IP	
16	J073237.5–133104	V667 Pup	07:32:37.5	-13:31:04	IP	
17	J074623.3–161341	SWIFT J0746.3–1608	07:46:23.3	-16:13:41	IP	Bernardini et al. (2019)
18	J075117.2+144421	PQ Gem	07:51:17.4	+14:44:25	IP	
19	J080108.2–462244	1RXS J080114.6–46232	08:01:17.0	-46:23:27	IP	Bernardini et al. (2017)
20	J083848.9–483125	IGR J08390-4833*	08:38:49.1	-48:31:25	IP	Revnivtsev et al. (2009b)
21	J095750.7–420838	SWIFT J0958.0–4208	09:57:50.6	-42:08:36	IP	Masetti et al. (2013) and Bernardini et al. (2017)
22	J101050.4–574648	IGR J10109-5746*	10:11:03.0	-57:48:15	SyS	Masetti et al. (2006a)
23	J114338.2+714121	DO Dra	11:43:38.3	+71:41:20	IP	
24	J121226.0-580023	IGR J12123-5802	12:12:26.2	-58:00:21	NL or IP?	Bernardini et al. (2013)
25	J123456.0–643400	RT Cru	12:34:54.7	-64:33:56	SyS	
26	J123816.3–384246	V1025 Cen	12:38:16.3	-38:42:46	IP	
27	J124853.5–624305	IGR J12489-6243	12:48:53.5	-62:43:05	CV?	Tomsick et al. (2012) and Fortin et al. (2018)
28	J125224.4–291457	EX Hya	12:52:24.4	-29:14:57	IP	
29	J140907.5–451717	V834 Cen	14:09:07.5	-45:17:17	AM	
30	J140846.0–610754	IGR J14091-6108*	14:08:46.0	-61:07:54	IP	Tomsick et al. (2016b)
31	J142507.7–611858	IGR J14257-6117*	14:25:07.6	-61:18:58	IP	Masetti et al. (2013) and Bernardini et al. (2018)
32	J145338.0–552223	IGR J14536-5522*	14:53:41.1	-55:21:39	AM	Masetti et al. (2006b)
33	J150918.8–665100	IGR J15094-6649*	15:09:26.0	-66:49:23	IP	Masetti et al. (2006b)
34	J152915.8–560947	IGR J15293-5609	15:29:15.8	-56:09:47	CV?	Tomsick et al. (2012); Fortin et al. (2018)
35	J154814.7-452840	NY Lup	15:48:14.7	-45:28:40	IP	
36	J155246.9–502953	IGR J15529-5029	15:52:46.9	-50:29:53	CV?	Tomsick et al. (2009)
37	J155930.2+255514	T CrB	15:59:30.2	+25:55:13	SyS	Masetti et al. (2008)
38	J161642.0–495700	IGR J16167-4957*	16:16:37.7	-49:58:44	IP	Masetti et al. (2006b)
39	J163553.8–472541	IGR J16358-4726	16:35:53.8	-47:25:41	SyS	Nespoli et al. (2008)
40	J165001.2–330658	IGR J16500-3307*	16:49:55.6	-33:07:02	IP	Masetti et al. (2008)
41	J165443.7–191630	IGR J16547-1916*	16:54:43.7	-19:16:31	IP	Masetti et al. (2010)
42	J170120.8–430531	IGR J17014-4306	17:01:28.2	-43:06:12	IP	Masetti et al. (2013); Bernardini et al. (2017)
43	J171236.5–241445	V2400 Oph	17:12:36.5	-24:14:45	IP	
44	J171930.0–410100	IGR J17195-4100*	17:19:35.9	-41:00:54	IP	Butters et al. (2008)
45	J172000.0–311600	IGR J17200-3116	17:20:05.9	-31:17:00	SyS?	Fortin et al. (2018)
46	J173024.0–060000	V2731 Oph*	17:30:21.5	-05:59:34	IP	Gaensicke et al. (2005)
47	J173159.8–191356	V2487 Oph	17:31:59.8	-19:13:56	Nova, IP?	Hernanz (2014)
48	J174017.7–290356	AX J1740.2–2903	17:40:16.1	-29:03:38	IP	Halpern and Gotthelf (2010)
49	J174026.9–365537	IGR J17404-3655	17:40:26.9	-36:55:37	CV or IP?	Clavel et al. (2019); Fortin et al. (2018)
50	J174624.0–213300	1RXS J174607.8–21333	17:46:03.2	-21:33:27	SyS	Masetti et al. (2008)
51	J174955.4–291920	CXOGBS J174954.5–294335	17:49:55.4	-29:19:20	IP	Johnson et al. (2017)
52	J175834.6–212322	IGR J17586-2129*	17:58:34.6	-21:23:22	SyS?	Fortin et al. (2018)
53	J180035.7+081106	V2301 Oph	18:00:35.8	+08:11:06	AM	
54	J180450.6–145450	IGR J18048-1455	18:04:39.0	-14:56:47	IP	Karasev et al. (2012); Middleton et al. (2012)
55	J180900.9–274214	IGR J18088-2741	18:09:01.0	-27:42:14	IP?	Tomsick et al. (2016a); Rahoui et al. (2017a)
56	J181504.0–105132	IGR J18151-1052	18:15:03.8	+10:51:35	IP?	Lutovinov et al. (2012); Masetti et al. (2013)
57	J181613.3+495204	AM Her	18:16:13.3	+49:52:04	AM	
58	J181722.2–250842	IGR J18173-2509*	18:17:22.3	-25:08:43	IP	Nichelli et al. (2009)
59	J181826.4–235248	IGR J18184-2352*	18:18:26.4	-23:52:48	CV?	Krivonos et al. (2017)
60	J182920.2–121251	IGR J18293-1213*	18:29:20.2	-12:12:51	IP?	Clavel et al. (2016)
61	J183049.9–123219	IGR J18308-1232*	18:30:49.9	-12:32:19	IP	Masetti et al. (2009)
62	J1832.3–0840	AX J1832.3–0840	18:32:19.3	-08:40:30	IP	Masetti et al. (2013)
63	J185502.2–310948	V1223 Sgr	18:55:02.2	-31:09:48	IP	
64	J190713.6–204554	V1082 Sgr*	19:07:13.7	-20:45:54	preCV	Tovmassian et al. (2018)
65	J192445.6+501414	CH Cyg	19:24:45.6	+50:14:14	SyS	
66	J192627.0+132205	IGR J19267+1325*	19:26:27.0	+13:22:05	IP	Evans et al. (2008)
67	J194011.5–102525	V1432 Aql	19:40:11.5	-10:25:25	AM	
68	J195511.0+004442	IGR J19552+0044	19:55:12.5	+00:45:37	pre-polar or IP	Bernardini et al. (2013); Tovmassian et al. (2017)
69	J195814.9+323018	V2306 Cyg	19:58:14.9	+32:30:18	IP	
70	J201531.4+371116	RX J2015.6+3711	20:15:31.4	+37:11:17	CV + blazar	Bassani et al. (2014)
71	J210933.8+432046	IGR J21095+4322	21:09:24.2	+43:19:36	CV?	Halpern et al. (2018)
72	J211352.8+542215	1RXS J211336.1+54222	21:13:35.4	+54:22:33	IP	Bernardini et al. (2017)
73	J212344.8+421802	V2069 Cyg	21:23:44.8	+42:18:02	IP	
74	J213330.0+510531	IGR J21335+5105*	21:33:30.0	+51:05:31	IP	

(*continued on next page*)

Table 1 (*continued*)

N	Source ID	Name	α_{2000}	δ_{2000}	Type	Ref
75	J214242.7 + 433509	SS Cyg	21:42:42.8	+ 43:35:10	DN	
76	J221755.4–082105	FO Aqr	22:17:55.4	-08:21:05	IP	
77	J225518.0–030943	AO Psc	22:55:18.0	-03:09:43	IP	
78	J232954.3 + 062811	EI Psc	23:29:54.3	+ 06:28:11	DN	

Note: * - discovered by *INTEGRAL*, IP - an intermediate polar, AM - a polar, type AM Her, DN - a dwarf Nova, NL - a Nova-like star, preCV - a precataclysmic CV, SyS - a symbiotic star, DDP - a double degenerate polar, a secondary star is also WD, LMXB - a low mass X-ray binary.

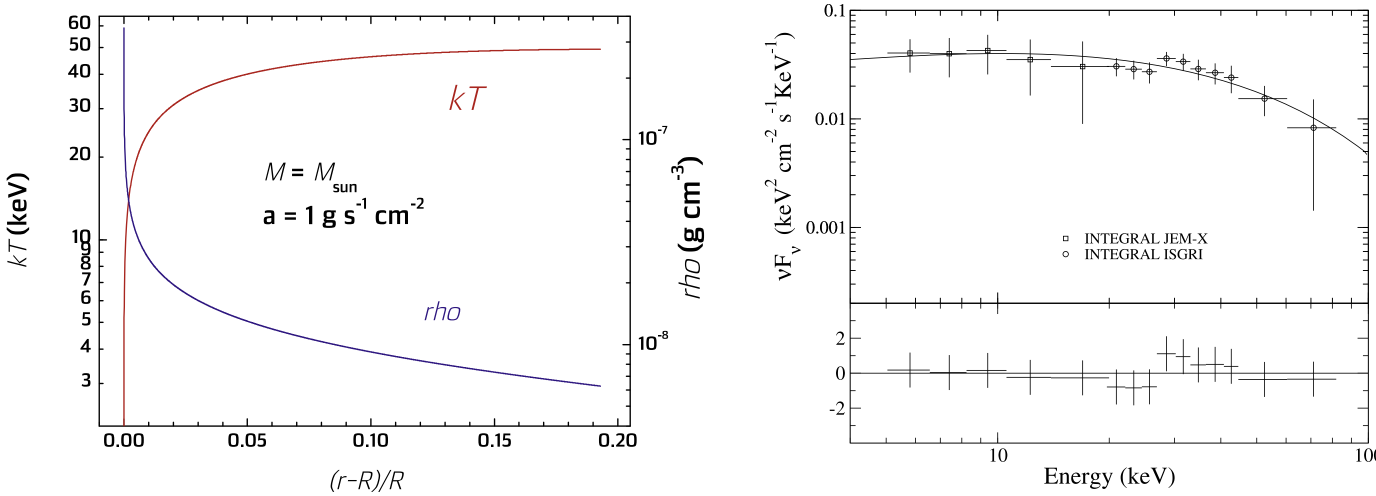

Fig. 1. Left: Distributions of temperature (red line) and density (blue line) in the model with $M = M_\odot$ and local mass accretion rate $a = 1$ g s^{-1} cm^{-2}. Right: The unfolded *INTEGRAL* JEM-X/ISGRI spectrum of V709 Cas with the best-fit post-shock model. Residuals between the data and model are shown below in units of sigma (from Falanga et al., 2005). (For interpretation of the references to colour in this figure legend, the reader is referred to the web version of this article.)

describes the optically thin PSR in the cylindrical geometry cooling only by a thermal radiation without a cyclotron one. We note that more physical and geometrical details should be included into the model to make it fully correct (see, e.g. the dipole geometry importance considered in Canalle et al. (2005), and the two-temperature plasma approach studied in Woelk and Beuermann (1996) and Saxton et al. (2007)). Nevertheless, even this simplest model is enough to describe adequately X-ray spectra in the hard energy band. An example of the PSR structure and spectrum of the bright IP V709 Cas, measured with *INTEGRAL*, are shown in Fig. 1.

This approach has been implemented in Suleimanov et al. (2005) (see also Suleimanov et al., 2016). In the simplest case the model spectrum can be computed as a sum of the local bremsstrahlung spectra. This is adequate to describe only the hard continuum above $\gtrsim$ 10 keV since the soft part of the observed spectra is dominated by spectral lines and photo-recombination continua. Therefore, the sum of the optically thin plasma spectra over the PSR height rather than multi-temperature bremstrahlung has to be used in this case. In addition, a complex absorption by intervening multiple partial covering neutral material further modifies the soft X-ray spectra of mCVs Mukai (2017). The detection of the fluorescent Fe K_α line at 6.4 keV indicates the presence of reflection from cold matter, either from the WD or the neutral pre-shock material, which should contribute in the continuum above 10 keV. Note that a significant Compton reflection component was found necessary in fitting high S/N spectra of bright IPs as observed by *NuSTAR* (Mukai et al., 2015; Wada et al., 2018).

To avoid the complications associated with the complex nature of the broadband X-ray spectra of IPs for the WD masses determination, it is reasonable, therefore, to restrict the modeling to the hard portion of the observed spectrum ($E > 15 - 20$ keV) (Hailey et al., 2016; Suleimanov et al., 2016, 2019).

Another complication, which may make WD mass estimates ambiguous, is a finite size of the magnetosphere which defines the height from which the material falls onto the surface. The free-fall velocity at the shock depends on the magnetospheric radius R_m, which is determined as the inner radius of the accretion disc disrupted by the WD magnetic field. Obviously in this case it is possible to determine only a combination of two values: the WD mass M and the relative magnetospheric radius $r_m = R_m/R$. As a consequence, a degeneracy between these two parameters appears. To break this degeneracy and estimate the WD mass, the magnetospheric radius needs to be evaluated independently. So far two approaches have been used to that avail. First, the corotational radius is the natural upper limit for R_m and can be used for the approximate estimate of the latter one. Another way is that in some cases the frequency of the break in the power spectrum of the given IPs can be measured, and this frequency is assumed equal to the Kepler frequency at the magnetospheric radius (see Revnivtsev et al., 2009b). The implementation of this approach is described in Suleimanov et al., 2016, 2019, and is available as the XSPEC model[2]. It is necessary to note, however, that the finite magnetospheric radius affects on the WD mass determination only in the case of the small magnetosphere size $r_m = R_m/R < 10$.

The hard X-ray radiation is also observed in non-magnetic CVs, e.g., in some dwarf novae during quiescence, and even Nova-like variables (see Table 1). The hard X-ray radiation in these systems originates from the optically thin boundary layer between fast rotating accretion flow and slow rotating WD (Pringle and Savonije, 1979; Tylenda, 1981; Narayan and Popham, 1993), or even from the optically thin part of the optically thick boundary layer Patterson and Raymond (1985). Spectra of the optically thin boundary layers are also well fitted with the cooling flow model (Done and Osborne, 1997). The generally accepted theory of boundary layers does not yet exist, and we will not describe here any details of different models.

It is important to note, however, that the maximum bremsstrahlung

[2] https://heasarc.gsfc.nasa.gov/xanadu/xspec/models/ipolar.html

temperature should correspond to the Keplerian velocity at the WD surface, rather than free-fall velocity. As a consequence, the maximum bremsstrahlung temperature has to be by factor of two smaller for the optically thin boundary layer in comparison with the post-shock temperature of a magnetic WD with the same mass. Therefore, the maximum bremsstrahlung temperature of the hard X-ray spectra of non-magnetic CVs can be used for WD mass estimations taking into account the remark above. The hard X-ray radiation of Symbiotic stars is believed to have similar origin as in non-magnetic CVs.

4. White dwarf masses in magnetized CVs according to the *INTEGRAL* measurements

The first estimate of a WD mass with *INTEGRAL* was made by Revnivtsev et al., 2004 using the bremsstrahlung temperature obtained from the approximation of the hard X-ray spectrum of the bright IP V1223 Sgr. Subsequently, *INTEGRAL* observations were used to estimate masses of several WDs using the PSR model and corresponding spectral model grid (Suleimanov et al., 2005). In particular, IBIS/ISGRI spectra were used together with the *RXTE* data to evaluate the WD mass in V2400 Oph (Revnivtsev et al., 2004); a combination of the IBIS/ISGRI data with JEM-X data was used to determine the WD mass in V709 Cas (Falanga et al., 2005). Later this model grid was used to estimate the WD masses in many IPs (see, e.g., Anzolin et al., 2009; Bernardini et al., 2012; Brunschweiger et al., 2009).

The extended *INTEGRAL* observations of CVs allowed to measure their hard X-ray spectra, which were fitted with the bremsstrahlung and power-law models (Barlow et al., 2006; Landi et al., 2009), but these were not used for the WD mass determination. We compiled all published WD mass measurements using the *INTEGRAL* data in Table 2. In line with the corresponding temperatures of the bremsstrahlung emission (Barlow et al., 2006; Landi et al., 2009), and for comparison, we also added the WD masses in some IPs recently determined using *NuSTAR* and *Swift*/BAT observations and more sophisticated PSR models (Suleimanov et al., 2019).

The comparison between the WD masses derived from *INTEGRAL* observations and the values taken from Suleimanov et al. (2019) are shown in Fig. 2, left panel. Most of the measurements well agree one with another within their 1σ uncertainties, with only two IPs, V2400 Oph and IGR J08390-4833, within 3σ.

As was mentioned above, one of the most straightforward ways to estimate the WD mass in IPs is to use the single bremsstrahlung temperature $kT_{\rm br}$ obtained from the simple fitting of their hard X-ray spectra. The simplest assumption in this approach is that the bremsstrahlung temperature equals to the maximum temperature of PSR $kT_{\rm sh}$ (see Eq. (1)). However, the averaged bremsstrahlung temperature has to be lower than $kT_{\rm sh}$, $kT_{\rm br} = A\,kT_{\rm sh}$, where $A < 1$. To obtain a real dependence of $kT_{\rm br}$ on the WD mass we show the bremsstrahlung temperatures of IPs, which were found in Landi et al., 2009, as a function of WD masses from Suleimanov et al. (2019) (Fig. 2, right). Note that we consider here only IPs with a well defined $kT_{\rm br}$, i.e. with the uncertainty on $T_{\rm br}$ smaller than $kT_{\rm br}/2$. The resulting dependence is well fitted with an approximate relation

$$kT_{\rm br} = A\,kT_{\rm sh} = \frac{A\,32\,M_1}{1.364\times(1-0.59\,M_1)}\ \ \text{keV}, \tag{2}$$

where $A = 0.52 \pm 0.03$. Here we used a linear fit for the $M-R$ relation (Suleimanov et al., 2016). The final expression for calculations of the WD mass using $kT_{\rm br}$ can be written as

$$M_1 = \frac{kT_{\rm br}}{A\times 23.46 + 0.59\,kT_{\rm br}}. \tag{3}$$

Note that this relation is correct for $M_1 < 1.2$ only, because the

Table 2
Observed and derived parameters of magnetic CVs.

N	Name	Type	M_1^a	$kT_{\rm br}^b$ (keV)	$kT_{\rm br}^c$ (keV)	M_1^e	Ref.
1	V1033 Cas*	IP	1.02 ± 0.15	> 14	15.9 ± 5.1	0.91 ± 0.15	Anzolin et al. (2009)
2	V709 Cas	IP	0.83 ± 0.04	$25.5^{+3.1}_{-2.7}$	23.3 ± 2.2	$0.82^{+0.12}_{-0.25}$	Falanga et al. (2005)
3	V515 And	IP	0.67 ± 0.07			0.79 ± 0.07	Bernardini et al. (2012)
4	GK Per	IP	0.79 ± 0.01	$43.7^{+128.8}_{-23.4}$	28.7 ± 15.7		
5	BY Cam	AM		$36.7^{+230.3}_{-22.7}$	14.8 ± 5.9	$> \mathbf{0.72}$	
6	MU Cam	IP	0.67 ± 0.08	$7.0^{+8.9}_{-3.8}$	8.1 ± 4.7		
7	IGR J08390-4833*	IP	1.27 ± 0.15			0.95 ± 0.08	Bernardini et al. (2012)
8	V834 Cen	AM		$18.7^{+61.0}_{-10.6}$	19.5 ± 7.8	$> \mathbf{0.5}$	
9	IGR J14536-5522*	IP		$14.0^{+5.4}_{-3.7}$	11.1 ± 4.6	$\mathbf{0.68 \pm 0.13}$	
10	IGR J15094-6649*	IP	0.85 ± 0.09	$18.8^{+11.5}_{-6.5}$	13.8 ± 5.1	0.89 ± 0.08	Bernardini et al. (2012)
11	NY Lup	IP	1.05 ± 0.04	$29.3^{+3.1}_{-2.7}$	27.1 ± 2.2		
12	IGR J16167-4957*	IP		$17.3^{+3.3}_{-2.7}$	13.2 ± 2.6	$\mathbf{0.77 \pm 0.07}$	
13	IGR J16500-3307*	IP	0.82 ± 0.09	$20.0^{+6.9}_{-4.7}$		0.92 ± 0.06	Bernardini et al. (2012)
14	IGR J16547-1916*	IP	0.83 ± 0.10			0.85 ± 0.15	Lutovinov et al. (2010)
15	V2400 Oph	IP	0.72 ± 0.05	$16.6^{+1.9}_{-1.7}$	18.6 ± 1.4	0.59 ± 0.05	Revnivtsev et al. (2004)
16	IGR J17195-4100*	IP	0.72 ± 0.06	$25.0^{+4.6}_{-3.6}$	27.0 ± 4.4	0.86 ± 0.06	Bernardini et al. (2012)
17	V2731 Oph*	IP	1.06 ± 0.03	$32.4^{+11.5}_{-8.1}$	26.7 ± 4.4	0.89 -1.02	de Martino et al. (2008)
18	V2487 Oph	IP?		$55.6^{+76.4}_{-24.5}$	25.5 ± 8.6	$> \mathbf{1.0}$	
19	2XMMi J180438.7–145647	IP			$(23.3^{+8.84}_{-5.9})^d$	$\mathbf{0.90^{+0.13}_{-0.11}}$	
20	IGR J18308-1232*	IP				0.85 ± 0.06	Bernardini et al. (2012)
21	V1223 Sgr	IP	0.72 ± 0.02	$17.7^{+1.6}_{-1.4}$	18.8 ± 1.2	0.71 ± 0.03	Revnivtsev et al. (2004)
22	V1432 Aql	AM		$24.4^{+15.3}_{-8.1}$	25.4 ± 7.0	$\mathbf{0.92 \pm 0.18}$	
23	V2069 Cyg	IP	0.83 ± 0.10	$19.2^{+12.3}_{-6.8}$	35.7 ± 16.8	0.82 ± 0.08	Bernardini et al. (2012)
24	IGR J21335+5105*	IP	0.95 ± 0.04	$23.6^{+5.0}_{-4.0}$	23.8 ± 4.3	0.93 ± 0.04	Anzolin et al. (2009)
25	FO Aqr	IP	0.57 ± 0.03	$29.7^{+70.1}_{-16.6}$			

Note: * – discovered by *INTEGRAL*, IP – an intermediate polar, AM – a polar, type AM Her, *a* – the WD masses from Suleimanov et al. (2019), *b* – $kT_{\rm br}$ from Landi et al. (2009), *c* – $kT_{\rm br}$ from Barlow et al. (2006), *d* – $kT_{\rm br}$ taken from Middleton et al. (2012), *e* – the WD masses obtained using INTEGRAL observations. The corresponding references are shown in the last column. The boldfaced WD masses given without references were obtained in this work using relation (3), and the bremsstrahlung temperatures measured in Landi et al. (2009), Barlow et al. (2006), and Middleton et al. (2012).

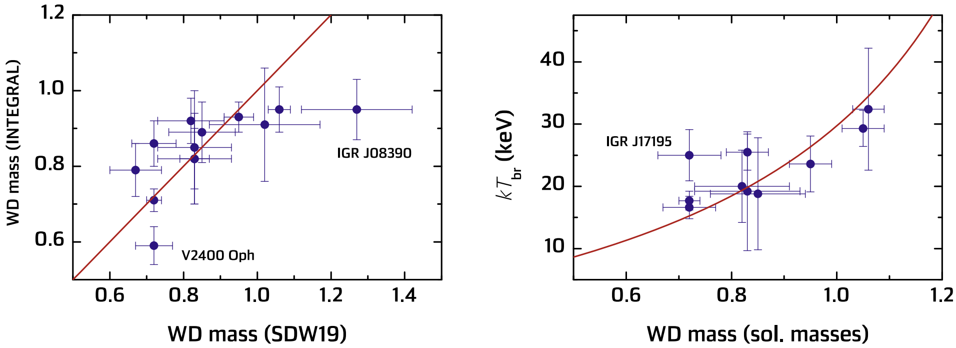

Fig. 2. Left: Comparison of the WD masses of the IPs determined using *INTEGRAL* data with those obtained by Suleimanov et al. (2019). Two outlier sources are marked. Right: Dependence of bremsstrahlung temperatures kT_{br} derived from the hard X-ray spectra of some IPs Landi et al. (2009) on the WD mass in these IPs Suleimanov et al. (2019). The red curve shows the fit of this dependence with the relation (2). (For interpretation of the references to colour in this figure legend, the reader is referred to the web version of this article.)

linear $M-R$ fit is not valid for larger masses. Nevertheless it represents a useful way for the quick WD mass estimates using only hard X-ray data.

Based on the relation (3) we estimated WD masses in three systems, the polar IGR J14536-5522, and the two IPs, IGR J16167-4957 and 2XMMi J180438.7–145647) with well determined bremsstrahlung temperatures. Worth mentioning is the estimated mass for the AM Her type system V1432 Aql (see Table 2) that is in remarkable agreement with that derived from *RXTE*/PCA data ($M_1 \approx 0.98$) by Ramsay (2000).

It is important to note that for some objects the bremsstrahlung temperatures kT_{br} reported in Landi et al., 2009 have large uncertainties, despite the relatively high brightness of these sources (Table 2). A possible reason of this is that their temperatures were determined using the spectra accumulated over a long time period (over five years). This implies that the large kT_{br} uncertainties for the brighter sources may be associated with the intrinsic variability of the spectrum related to mass accretion rate variations, which, in turn, lead to the variations of the magnetospheric radius. For these objects only lower limits on their WD masses are reported in Table 2, if any other WD mass determinations are absent. Thus, these systems require additional dedicated investigations to draw conclusions regarding the masses of their WD primaries.

5. Symbiotic stars

Symbiotic stars, long-period binary systems where either a white dwarf or a neutron star accretes from the wind of a red giant companion, have been known as X-ray sources since the70′s (Allen, 1981; Anderson et al., 1981; Cordova et al., 1981; Lewin et al., 1971). The characteristics of the X-ray emission from symbiotic stars were compiled by Muerset et al. (1997) using *R*OSAT data.

Symbiotic stars were classified according to the following scheme (see Muerset et al., 1997 and following development by Luna et al. (2013)):

α: supersoft X-ray sources. Most of their X-ray radiation is emitted below $\approx$ 0.4 keV. They are supposed to be white dwarfs with a quasi-steady shell burning on their surface;
β: soft X-ray sources. Their X-ray spectra extend up to $\approx$ 2.4 keV (i.e., the upper bound of the *ROSAT*energy range). The X-ray photons are likely produced by the collisions of the winds from the white dwarf and the red giant;
γ: symbiotic stars with accreting neutron stars (or X-ray symbiotic stars). They have the hard X-ray emission ($E \gtrsim 2.4$ keV), mostly from the optically thick Comptonizing plasma;
δ: hard X-ray sources with high absorption. They show a strong thermal emission above $E \approx 2.4$ keV, likely originating in the accretion disc boundary layer;
β/δ: symbiotics with soft and hard thermal components. They have properties in common with the subclasses *β* and *δ*, and the mechanisms producing both spectral components are supposed to be the same of those proposed for *β* and *δ* sources.

Only two systems with neutron stars as accreting object were present in the compilation by Muerset et al. (1997): GX 1 + 4 and Hen 3-1591. In the modern era of instruments sensitive to energies of more than 10 keV such as *INTEGRAL* and *Swift*/BAT, about 10 more similar systems have been discovered. It is believed that their X-ray emission arises from an optically thick Comptonizing plasma with no emission lines (see Marcu et al., 2011). These systems are out of scope of the current review and will be reviewed separately in this volume.

The vast majority of symbiotic systems host, however, accreting WDs, making them long-period relatives of CVs. After the aforementioned compilation by Muerset et al. (1997) and Luna et al. (2013) reported the first detection of the X-ray emission from eight more symbiotic systems using *Swift*/XRT, thus bringing the total number of known symbiotic systems as X-ray sources to 33 (see also Mukai, 2017).

Four systems stood out from this sample, RT Cru, T CrB, CD -57 3057 and CH Cyg, because of their unprecedented high energy emission. The prototype of them is RT Cru, which was first detected with *INTEGRAL*/IBIS in 2003–2004 with the name of IGR J12349-6434 at a $\sim$ 3 mCrab level in the 20–60 keV energy band (Chernyakova et al., 2005). Later, *INTEGRAL* detected RT Cru again in 2012 with a flux of $\sim$ 13 mCrab in the 18–40 keV band (Sguera et al., 2012), and in 2015 at the level of $\sim$ 6 mCrab in the 22–60 keV band (Sguera et al., 2015). The joint *Swift*/XRT + *INTEGRAL* JEM-X/IBIS/ISGRI spectrum from RT Cru is shown in Fig. 3. The system CD -57 3057 was also registered with *INTEGRAL* during the Crux Galactic arm survey as the IGR J10109-5746 source (Revnivtsev et al., 2006b). Moreover, *INTEGRAL* discovered several new hard X-ray sources, which are considered symbiotic star candidates. The full list of such sources can be found in *INTEGRAL* catalogues, but here we can mention the most promising objects: IGR J15293-5609 (= CXOU J152929.3–561213) (), IGR J17164-3803 (Rahoui et al., 2017b) and IGR J17463-2854 (Karasev et al., 2015).

Because of their hard X-ray emission, these objects were dubbed as *δ*-type X-ray sources in Luna et al. (2013). This hard X-ray emission appears to be thermal, and the X-ray spectrum can be modeled with a highly absorbed cooling flow model (see Section 3) with maximum temperatures of about 50 keV (Eze et al., 2010; Luna and Sokoloski, 2007; Smith et al., 2008). Such hard X-ray emission most likely originates in the most internal region of the accretion disk, the boundary layer, which is optically thin to its own radiation if the accretion rate is low, $\dot{M} \lesssim 3 \times 10^{-10}$ $M_{\odot}$ yr^{-1} for a 1 $M_{\odot}$ white dwarf (Popham and Narayan, 1995; Suleimanov et al., 2014). Conversely, the hard X-rays could arise in the accretion column of a magnetic WD, similarly to IPs, although the WD period has not been detected yet in any system (Ducci et al., 2016).

Nevertheless, most of the accretion-powered, hard X-rays emitting, symbiotic systems are too weak to be detected with the current instruments ($L_X \leq 10^{34}$ ergs s^{-1}). However, Luna et al. (2013) found that the amplitude of the flickering in the UV band, with time scales of minutes to hours, (see Fig. 4) is greater in those systems with harder X-ray emission, while sources with low-amplitude UV flickering tend to

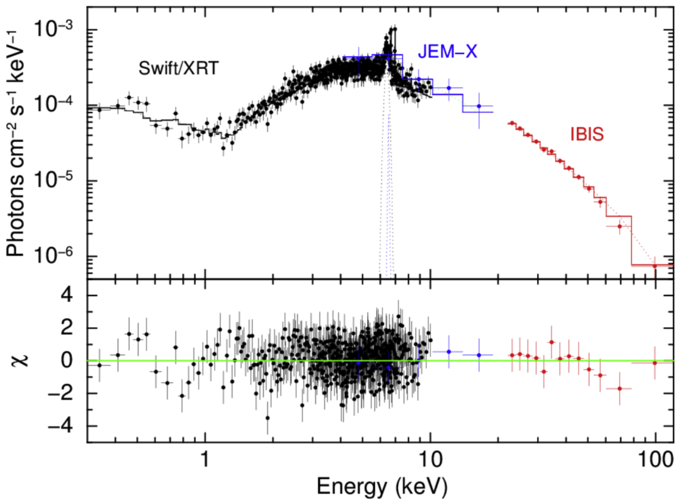

Fig. 3. Combined *Swift*/XRT (black), JEM-X (blue), IBIS/ISGRI (red) unfolded spectra of RT Cru/IGR J12349-6434. The *INTEGRAL* spectrum was constructed accumulating data from 2003 January 29, and 2014 December 20, while for *Swift*/XRT the spectrum was built accumulating data from Aug 20, 2005 to Dec 24, 2012 (see Ducci et al., 2016, for details). (For interpretation of the references to colour in this figure legend, the reader is referred to the web version of this article.)

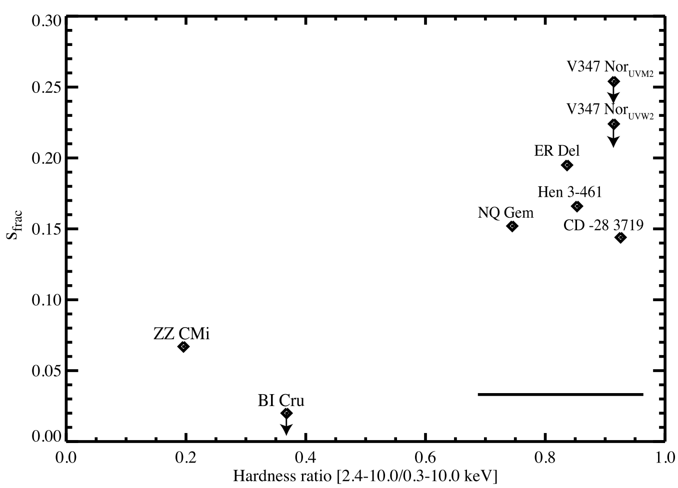

Fig. 4. Fractional rms amplitude of flickering (S_{frac}) vs. hardness ratio in X-rays. Objects with harder X-ray emission tend to have more intense UV flickering. Downward arrows indicate upper limits. The average error bar is shown at the bottom-right corner (from Luna et al., 2013).

have relatively little emission above 2 keV. This provides a tool to search for accretion-powered systems while hard X-ray observation would be unfeasible long.

As in the case of IPs, the post-shock maximum temperature can be used to determine the WD mass if the X-rays arise in a completely optically thin boundary layer, otherwise, the maximum temperature provides a lower limit for the WD mass. The best-studied systems, RT Cru and T CrB, show strong, long-term variability in their X-ray light curves, which points to changes in the accretion rate and subsequently in the optical depth of the boundary layer.

In the standard accretion disk theory, the total accretion luminosity is divided in equal portions between the Keplerian portion of the accretion disk and the boundary layer. The Keplerian accretion disk radiates mostly in the UV and optical regimes while the boundary layer does it in X-rays. Thus, the ratio of L_{UV}/L_X should be equal to one if the boundary layer is completely optically thin. During the high-accretion-rate episodes, such as those in dwarf novae in outburst, or persistent high-accretion regimes as in novae-like, the boundary layer often becomes optically thick to its own radiation, and the peak of its emission shifts toward longer wavelengths, causing the L_{UV}/L_X ratio to be significantly greater than one.

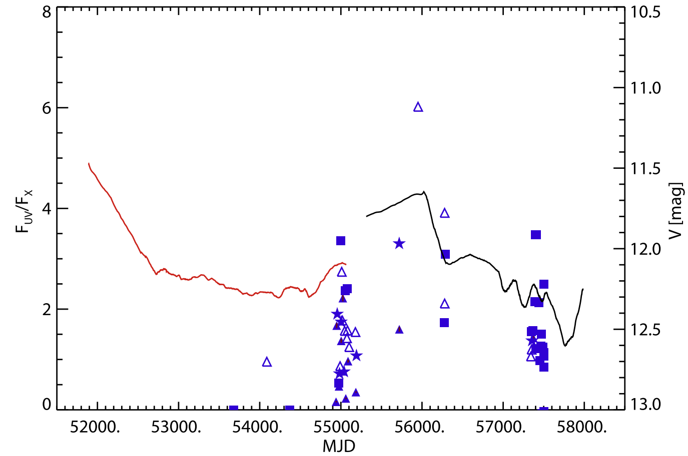

Fig. 5. (*Left-hand Y-axis*) Ratio of reddening-corrected *Swift*/UVOT magnitudes (U: filled triangle; W1: star; M2: open triangle; W2: square) over unabsorbed X-ray flux in the 0.3–80 keV band for each *Swift* observation of RT Cru. (*Right-hand Y-axis*) Over-plotted are the ASAS (red solid line) and AAVSO (black solid line) V-band light curve, smoothed for clarity Luna et al. (2018). (For interpretation of the references to colour in this figure legend, the reader is referred to the web version of this article.)

Multiwavelength, UV and X-rays light curves obtained with *Swift*/XRT and UVOT can be used to trace the optical depth of the boundary layer. Luna et al., 2018 used data from the *Swift*/XRT and UVOT simultaneously and found that, in RT Cru, the L_{UV}/L_X is greater than one during the optical maximum while it is closer to one during the optical minimum (Fig. 5). This behavior might be related with the putative orbital period of about 4000 days found in the optical and *Swift*/BAT light curves.

Another interesting case is that of T CrB, a symbiotic recurrent nova with a recurrence period of about 80 years. The last thermonuclear outburst happened in 1946. Given that it is the closest recurrent nova, it will certainly produce copious hard-X-rays-to-γ rays during the next thermonuclear outburst that could be detected with *INTEGRAL*.

Since 2014, T CrB entered in what has been called a ”super-active” state (Munari et al., 2016), in which the optical brightness increased by about 1 magnitude, the 15–50 keV flux almost vanished, the UV flux increased by a factor of about 40 and a new soft X-ray (0.3-1 keV) black body type component emerged. This phenomenology is akin to what is observed during the dwarf nova outbursts, in which the most internal region of the accretion disk changes its optical depth in response to an increase in the accretion rate. However, given the large size of the accretion disk in T CrB, these changes happen in a far longer time scale.

6. Luminosity function of CVs

The determination of the space densities of different classes of CVs in the Galaxy is essential to constrain models of CV formation and evolution. Although fairly large catalogues of CVs, mainly selected in the optical band, have been available for a long time (see Ritter and Kolb, 2003 and references therein), they were not well suited for determining CV space densities because of the strong and poorly understood selection effects Patterson (1984), see also Goliasch and Nelson (2015). A breakthrough occurred when the *ROSAT* observatory conducted an all-sky soft X-ray survey and provided a well-defined, flux limited sample of ~ 50 CVs (mainly identified among the X-ray sources from the *ROSAT* Bright Survey at high Galactic latitudes, $|b| > 30°$), which has then been used to estimate the space density of non-magnetic and magnetic CVs (Schwope et al., 2002; Pretorius and Knigge, 2012; Pretorius et al., 2013). Recently, an additional small sub-sample of CVs was identified among the X-ray sources detected in deeper pointed observations with *ROSAT*, which made it possible to extend the soft X-ray luminosity function of CVs down to 10^{29} erg s^{-1} (Burenin et al., 2016). However, the *ROSAT* survey was limited to energies below 2 keV, whereas, as discussed in depth in this review, some classes of CVs such as IPs, emit a large or even dominant fraction of their bolometric luminosity at higher energies. Therefore, in order to conduct a reliable census of such objects it is highly desirable to select them in the hard X-ray band. The first representative sample of CVs selected in a moderately hard X-ray band, 3–20 keV, was obtained by Sazonov et al. (2006) based on the *Rossi XTE* Slew Survey (XSS) (Revnivtsev et al., 2004b). This sample consisted of 24 known CVs, including 4 non-magnetic ones (dwarf novae), 19 magnetic ones (6 polars and 13 intermediate polars) and 1 symbiotic star. For all but one of these objects, distance estimates were available (including several accurate parallax measurements), with most of them located within 500 pc from the Sun. This sample was used to construct the 3–20 keV luminosity function of CVs spanning three decades in luminosity (from 10^{31} to 10^{34} erg s^{-1}) and to measure the total space density and total X-ray luminosity density (per unit stellar mass) of such objects: $(4.8 \pm 1.6) \times 10^{-7}$ pc^{-3} and $(2.4 \pm 0.6) \times 10^{27}$ erg s^{-1} $M_\odot^{-1}$ (3–20 keV), respectively. A relevant study was later performed by Byckling et al. (2010), where *Suzaku, XMM-Newton* and *ASCA* data were used to construct a 2–10 keV luminosity function of dwarf novae and it was shown that this subclass of CVs contributes $\sim 16\%$ to the total local X-ray luminosity density of CVs.

Afterwards, Revnivtsev et al. (2008) applied the same approach to the data of *INTEGRAL* observations and for the first time constructed a sample of CVs selected in a truly hard X-ray band, 17–60 keV. To this end, they used the catalogue of sources detected by the IBIS instrument over the whole sky during the first 3.5 years of the *INTEGRAL* mission (Krivonos et al., 2007b). The sample consisted of 17 CVs: 15 intermediate polars (note that the JEM-X telescope aboard *INTEGRAL* has detected 3 of these objects also in the 5–10 and 10–25 keV energy bands, Grebenev and Mereminskiy (2015)), one dwarf nova, and one classical nova (V2487 Oph, which also could be a magnetic CV of the IP type Hernanz (2014)). As in previous studies, a serious problem was posed by the highly uncertain distances to some of the studied objects. If the spectral type of the secondary star and the apparent brightness of a CV are known, one can usually attempt to estimate its distance. However, in the case of IPs, the accuracy of this method is significantly affected by the fact that the optical light is mainly produced by the accretion disc rather than the secondary star. Detailed spectroscopic information allows one in some cases to determine the contribution of the light of the companion star to the optical brightness of the binary, but this information was not available for all CVs in the *INTEGRAL* sample. To overcome these difficulties, the authors took the following novel approach: they measured the correlation between the orbital period and the hard X-ray luminosity for the six CVs with known distances from the sample and used the derived empirical, but physically motivated dependence to predict the hard X-ray luminosities and hence distances for the remaining objects.

The resulting *INTEGRAL* sample, despite its relatively small size, effectively covered three orders of magnitude in luminosity, 10^{32}–10^{35} erg s^{-1} (in addition, the absence of sources in the 10^{31}–10^{32} erg s^{-1} provided an interesting upper limit on the space density of such objects), which made it possible to construct the luminosity function of CVs in the hard X-ray band for the first time (Fig. 6). The integrated space density of CVs with hard X-ray luminosities above 10^{32} erg s^{-1} proved to be $(1.5 \pm 0.6) \times 10^{-7}$ pc^{-3} near the Sun, or equivalently $(3.8 \pm 1.5) \times 10^{-6}$ $M_\odot^{-1}$ (taking into account the local stellar density ~ 0.04 $M_\odot$ pc^{-3}). The total X-ray luminosity density of such objects was found to be $(1.3 \pm 0.3) \times 10^{27}$ erg s^{-1} $M_\odot^{-1}$ (17–60 keV). Finally, it proved possible to estimate the exponential scale height of CVs (primarily IPs) in the Galactic disc at 130^{+93}_{-46} pc.

A similar study has been subsequently carried out using the data of the all-sky hard X-ray survey conducted by the BAT instrument aboard the *Swift* observatory (Pretorius and Mukai, 2014). The authors imposed selection cuts in flux (above 2.5×10^{-11} erg cm^{-2} s^{-1} at 14–195 keV) and Galactic latitude ($|b| > 5^\circ$) and obtained a sample of 19 CVs, including 15 IPs. The latter sub-sample was used to obtain an estimate of the local space density of IPs with hard X-ray (14–195 keV) luminosities above 10^{32} erg s^{-1}: $1^{+1}_{-0.5} \times 10^{-7}$ pc^{-3}, in excellent agreement with the *INTEGRAL* measurement.

The recent second release (DR2) of *Gaia* parallaxes (Collaboration, 2018) now offers the opportunity to assess the true space densities and determine more accurate luminosity function. A first work using the shallow flux-limits of the 70-month *Swift*/BAT sample by Pretorius and Mukai (2014) and *Gaia* parallaxes, the IP space density is found to be lower than previously estimated with an upper limit of $< 1.3 \times 10^{-7}$ pc^{-3} although consistent within errors with previous determinations Schwope (2018). A lower CV space density than predicted by most binary population synthesis models has been recently confirmed by Pala et al. (2019) using a volume limited sample of 42 CVs within 150 pc. They also find that the fraction of mCVs is very large $\sim 33\%$. It is therefore crucial to extend the study to the larger fraction of mCVs detected so far. In this respect it is worth mentioning the successful launch of the Russian-German *Spectr-RG* mission in summer 2019. The eROSITA and ART-XC telescopes on board of this mission (Merloni et al., 2012; Pavlinsky et al., 2018) will conduct the most sensitive X-ray survey in the 2–11 keV band to date, and thus promise the discovery of thousands of faint sources pushing the limits of current X-ray luminosity function and assessing the true CV space densities.

7. Galactic ridge X-ray emission

There are two major large-scale extended diffuse features in the X-ray sky (above 2 keV): the highly isotropic cosmic X-ray background (CXB) and an emission concentrated towards the Galactic plane – the Galactic ridge X-ray emission (GRXE) (Warwick et al., 1985; Worrall et al., 1982). While it became clear long ago that the CXB is a superposition of numerous active galactic nuclei, the origin of the GRXE remained a puzzle for a long time.

The GRXE energy spectrum contains a number of emission lines of highly ionized heavy elements indicating that the radiation originates in an optically thin plasma with a temperature $\sim 10^8$ K (Koyama et al., 1986; Tanaka, 2002). The total GRXE luminosity is $\sim (1–2) \times 10^{38}$ erg s^{-1} (Valinia and Marshall, 1998). Historically, two points of view were confronted: (i) the GRXE is the superposition of point-like sources or (ii) it is truly diffuse emission. Each of these hypotheses had its problems. The proponents of the former usually tried to account for the observed GRXE luminosity in terms of the expected contributions from different known classes of faint ($L_X < 10^{34}$ erg s^{-1}) point sources, but the space densities involved in this estimation were not known accurately enough to draw firm conclusions (Worrall and Marshall, 1983; Ottmann and Schmitt, 1992; Mukai and Shiokawa, 1993). The main difficulty with the second scenario was to explain how to keep the hot plasma within the Galaxy or, if it is outflowing, to find the source of energy maintaining this strong wind (Tanaka, 2002).

In 2006, Revnivtsev et al. (2006a) accomplished a crucial achievement by demonstrating that the GXRE surface brightness, as mapped in the 3–20 keV energy band by *RXTE*, closely traces the near-infrared (NIR) surface brightness of the Milky Way and hence the distribution of stars throughout the Galaxy. This strongly suggested that the GXRE consists of point-like stellar-type sources. The measured X-ray/NIR correlation implied that the cumulative specific X-ray emissivity of these unresolved X-ray sources is $(3.5 \pm 0.5) \times 10^{27}$ erg s$^{-1}M_\odot^{-1}$ (3–20 keV).

The same team (Sazonov et al., 2006) used the *RXTE* data to

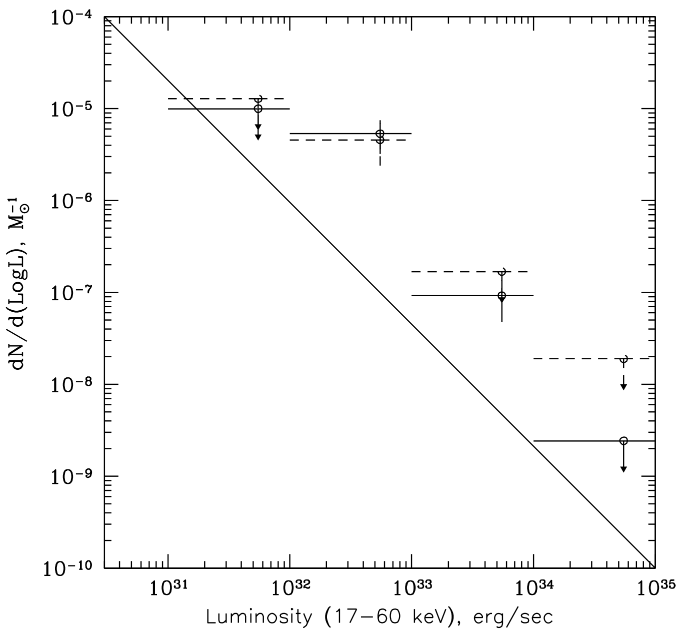

Fig. 6. Luminosity function of CVs detected by *INTEGRAL* over the whole sky (solid crosses). The dashed crosses show the luminosity function obtained excluding the Galactic plane region ($|b| < 5^\circ$), where there remain unidentified *INTEGRAL* sources. From (Revnivtsev et al., 2008).

construct the luminosity function of CVs (see Section 6) and coronally active binary stars (ABs, of RS CVn and other types), in the Solar neighbourhood, which allowed them to determine the integrated 3–20 keV luminosity of such faint ($L_X < 10^{34}$ erg s^{-1}) X-ray sources per unit stellar mass: $(5.3 \pm 1.5) \times 10^{27} M_\odot^{-1}$ erg s^{-1}. Remarkably, this locally measured quantity proved to be consistent, within the uncertainties, with the X-ray production rate required to explain all of the GRXE (see above). Furthermore, the spatial distribution of CVs and ABs is expected to trace the overall distribution of stars in the Galaxy. Therefore, a consistent picture emerged that the bulk of the GRXE is made up by ABs and CVs. This conclusion has later received a spectacular confirmation from the direct resolution of $\sim$ 80% of the GRXE at 6–8 keV into discrete sources in ultra-deep *Chandra* observations of a small region near the Galactic Centre (Revnivtsev et al., 2009a; 2011).

If the GRXE indeed represents the sum of the emissions from ABs and CVs, then also the shape of its energy spectrum must be a superposition of representative spectra of these classes of objects. The hard X-ray spectrum has always been a major issue in the study of the GRXE. In particular, if it had a power-law shape, it would imply that non-thermal phenomena, such as cosmic-ray induced emission (Skibo et al., 1997), are involved in the formation of the GRXE. The IBIS telescope aboard *INTEGRAL* has for the first time combined a large field of view with moderate angular resolution, making it possible to measure the GRXE spectrum by collecting a significant flux of Galactic "diffuse" hard X-rays and separating out the contribution of bright point sources.

Already early studies based on the IBIS observations showed that the GRXE spectrum does not extend into the gamma-ray range from the X-ray band with the same slope (Lebrun et al., 2004; Terrier et al., 2004). A later, in-depth investigation (Krivonos et al., 2007a) demonstrated that: (i) the GRXE hard X-ray (17–60 keV) surface brightness is proportional to the NIR surface brightness of the Milky Way (Fig. 7), just like the softer (3–20 keV) emission, (ii) the inferred GRXE emissivity per unit stellar mass in the 17–60 keV energy band is (0.9–1.2) $\times$ 10^{27} erg s$^{-1}M_\odot^{-1}$, in excellent agreement with the 17–60 keV luminosity density of CVs in the Solar neighborhood (see the preceding section), and (iii) there is a pronounced cutoff in the GRXE spectrum above 20–30 keV. A comparison of the measured GRXE spectrum with the sum of the expected contributions of different classes of faint X-ray sources, weighted according to their relative contributions to the local X-ray luminosity density, showed an excellent agreement (Fig. 8). The *INTEGRAL* observations have thus provided

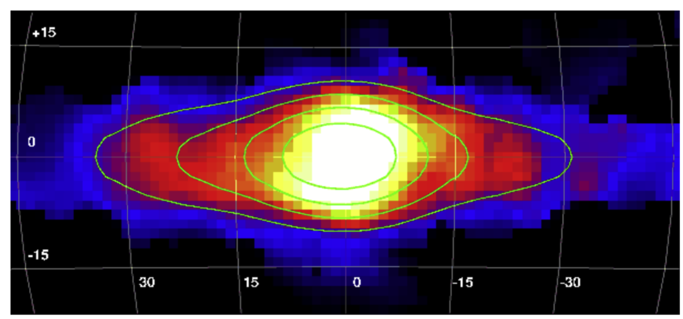

Fig. 7. Map of the unresolved Galactic hard X-ray (17–60 keV) emission obtained with *INTEGRAL*/IBIS, in comparison with the NIR intensity contours from *COBE*/DIRBE. Colors indicate different intensities of the hard X-ray emission, approximately from 0 to 150 mCrab. See details in (Krivonos et al., 2007a).

strong additional support to the GRXE being the integrated emission of ABs (dominating at energies below $\sim$ 5 keV) and CVs (dominating between $\sim$ 5 and $\sim$ 50 keV), mainly IPs.

The position of the high-energy cutoff in the GRXE spectrum measured by *INTEGRAL* can be directly linked to the maximal (virial) temperature of the X-ray emitting plasma (see Section 3) near the surface of the accreting magnetic WDs composing the GRXE. Based on this idea and the PSR model spectra from Suleimanov et al. (2005), Krivonos et al. (2007a) estimated the average mass of such objects in the Galaxy to be $\sim$ 0.5–0.6 $M_\odot$. A similar value, 0.6–0.7 $M_\odot$, was obtained in Yuasa et al. (2012) based on *Suzaku* GRXE observations.

Recently, unresolved extended hard X-ray (20–40 keV) emission has been detected by *NuSTAR* in the inner few parsecs of the Galaxy (Perez et al., 2015). Resolved hard X-ray point sources have been further identified in the *NuSTAR* survey of 0.6 deg^2 Galactic Center region (Hong et al. (2016). As demonstrated by (Hailey et al., 2016), the most natural interpretation of this signal is integrated emission from a large population of IPs in this region. Interestingly, the inferred typical mass of the WDs in these systems, $\sim$ 0.9 $M_\odot$, is somewhat higher than that estimated for the whole Galaxy from the *INTEGRAL* observations of the GRXE (see above), which urges further investigation. However, it is worth noticing that the high mass value is however not so different from that of normal CVs (Zorotovic et al. (2011)). We note in this connection that the average WD mass in nearby bright IPs (0.8–0.9 $M_\odot$,

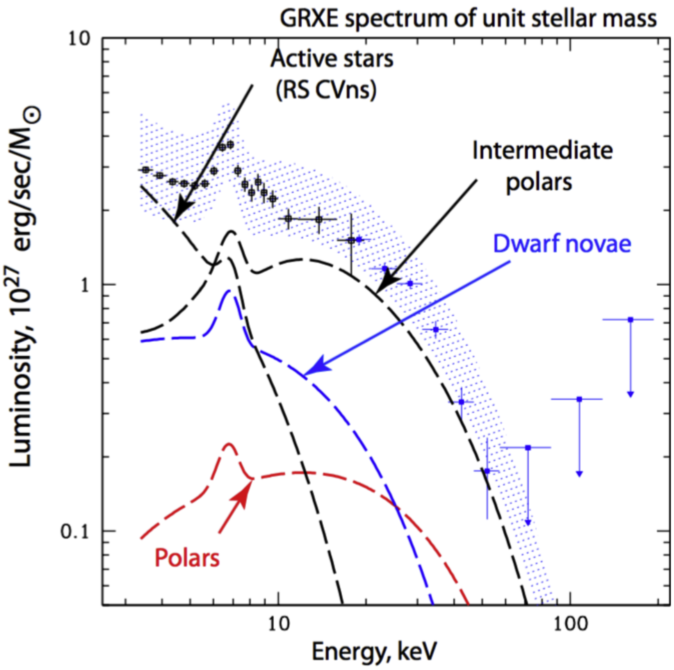

Fig. 8. GRXE spectrum measured with *RXTE*/PCA (open black squares) and *INTEGRAL*/IBIS data (filled blue squares), in comparison with typical spectra of the X-ray source classes expected to significantly contribute to the GRXE. These spectra are plotted with normalizations corresponding to their expected relative contributions to the GRXE (derived from the local statistics of faint X-ray sources (Sazonov et al., 2006)). The shaded region shows the sum of these spectra with the associated uncertainties. From (Revnivtsev et al., 2007). (For interpretation of the references to colour in this figure legend, the reader is referred to the web version of this article.)

see Suleimanov et al., 2019; Yuasa et al., 2010; de Martino, Bernardini, Mukai, Falanga, Masetti) is close to the value found in Hailey et al. (2016).

8. Conclusions

The contribution of the *INTEGRAL* observatory in the investigations of hard X-ray sky is very significant. The surveys of the Galactic plane and the Galactic center provide a lot of new information about known X-ray sources and allow to discover many new sources. Accreting white dwarfs in close (CVs) and wide (SySs) binary systems were also extensively studied with INTEGRAL. Here we have described the main results obtained with *INTEGRAL* in this field.

We presented the identified accreting WDs observed with *INTEGRAL* until November 2019 although many new identifications will further increase this class of hard X-ray emitting galactic sources. The most numerous CVs among them are of the IP type. *INTEGRAL* discovered 21 new CVs and SySs, including candidates, and the observed X-ray spectra were used for the determination of the WD masses in 18 bright IPs and polars. The WD masses in four sources were also estimated in this review for the first time. We also discussed the contribution of the *INTEGRAL* observatory in the study of symbiotic stars.

The *INTEGRAL* CV sample has permitted the first measurement of the hard X-ray (17–60 keV) luminosity function of CVs in the Solar neighborhood between 10^{32} and 10^{34} erg s^{-1} (and stringent upper limits on the CV space density at 10^{31}–10^{32} and 10^{34}–10^{35} erg s^{-1}) and of the total hard X-ray luminosity density of nearby CVs (dominated by IPs): $(1.3 \pm 0.3) \times 10^{27}$ erg s^{-1} $M_\odot^{-1}$ (17–60 keV). Thanks to the good coverage of the Galactic plane and bulge regions by *INTEGRAL* observations, it has been demonstrated that the Galactic unresolved hard X-ray emission (from the Galactic Ridge) closely follows the distribution of stars in the Milky Way, with the inferred emissivity per unit stellar mass in the 17–60 keV energy band of $(0.9–1.2) \times 10^{27}$ erg $s^{-1}M_\odot^{-1}$. The excellent agreement with the aforementioned hard X-ray luminosity density of nearby CVs implies that the GRXE is mainly produced by IPs and other CVs at hard X-ray energies. This conclusion has been further strengthened by the measurement of the GRXE energy spectrum with *INTEGRAL*, which revealed a cutoff above 20–30 keV as expected from it being the superposition of CV spectra.

Declaration of Competing Interest

The authors have no conflict of interest.

Acknowledgements

This review was supported by several programs and grants. AL, VS and VD acknowledge a support from the Russian Science Foundation, project 19-02-00423. GJML acknowledges financial support from grants ANPCYT-PICT 0478/14, PICT 0901/2017. DdM acknowledges financial support from ASI-INAF contracts I/037/12/0 and.2017-14-H.0 and INAF-PRIN SKA/CTA Presidential Decree 70/2016 and INAF ”Sostegno alla ricerca scientifica main streams dell'INAF”, Presidential Decree 43/2018. LD acknowledges grant 50 OG 1902. The work of VS was also supported by the DFG grant WE 1312/51-1.

References

Aizu, K., 1973. X-Ray Emission region of a white dwarf with accretion. Progr. Theor. Phys. 49 (4), 1184–1194. https://doi.org/10.1143/PTP.49.1184.
Allen, D.A., 1981. X-Ray observations of symbiotic stars. MNRAS 197, 739–743. https://doi.org/10.1093/mnras/197.3.739.
Anderson, C.M., Cassinelli, J.P., Sanders, W.T., 1981. X-ray detection of the symbiotic star AG Dra. ApJ 247, L127–L130. https://doi.org/10.1086/183605.
Anzolin, G., de Martino, D., Falanga, M., Mukai, K., Bonnet-Bidaud, J.-M., Mouchet, M., Terada, Y., Ishida, M., 2009. Broad-band properties of the hard X-ray cataclysmic variables IGR J00234 + 6141 and 1RXS J213344.1 + 510725. A&A 501 (3), 1047–1058. https://doi.org/10.1051/0004-6361/200911816.
Balman, S., Revnivtsev, M., 2012. X-ray variations in the inner accretion flow of dwarf novae. A&A 546, A112. https://doi.org/10.1051/0004-6361/201219469.
Barlow, E.J., Knigge, C., Bird, A.J., J Dean, A., Clark, D.J., Hill, A.B., Molina, M., Sguera, V., 2006. 20-100 keV properties of cataclysmic variables detected in the INTEGRAL/IBIS survey. MNRAS 372 (1), 224–232. https://doi.org/10.1111/j.1365-2966.2006.10836.x.
Bassani, L., Landi, R., Malizia, A., Stephen, J.B., Bazzano, A., Bird, A.J., Ubertini, P., 2014. The counterpart/s of IGR J20159 + 3713/SWIFT J2015.9 + 3715: dissecting a complex region with emission from kev to TeV. A&A 561, A108. https://doi.org/10.1051/0004-6361/201322292.
Beardmore, A.P., Osborne, J.P., Hellier, C., 2000. The multi-temperature X-ray spectrum of the intermediate polar V1223 Sagittarii. MNRAS 315 (2), 307–315. https://doi.org/10.1046/j.1365-8711.2000.03477.x.
Bernardini, F., de Martino, D., Falanga, M., Mukai, K., Matt, G., Bonnet-Bidaud, J.-M., Masetti, N., Mouchet, M., 2012. Characterization of new hard X-ray cataclysmic variables. A&A 542, A22. https://doi.org/10.1051/0004-6361/201219233.
Bernardini, F., de Martino, D., Mukai, K., Falanga, M., 2018. IGR J14257-6117, a magnetic accreting white dwarf with a very strong strong X-ray orbital modulation. MNRAS 478 (1), 1185–1192. https://doi.org/10.1093/mnras/sty1090.
Bernardini, F., de Martino, D., Mukai, K., Falanga, M., 2019. The true nature of Swift J0746.3-1608: a possible intermediate polar showing accretion state changes. MNRAS 484 (1), 101–106. https://doi.org/10.1093/mnras/sty3499.
Bernardini, F., de Martino, D., Mukai, K., Falanga, M., Andruchow, I., Bonnet-Bidaud, J.-M., Masetti, N., Buitrago, D.H.G., Mouchet, M., Tovmassian, G., 2013. On the nature of the hard X-ray sources SWIFT J1907.3–2050, IGR J12123-5802 and IGR J19552 + 0044. MNRAS 435 (4), 2822–2834. https://doi.org/10.1093/mnras/stt1434.
Bernardini, F., de Martino, D., Mukai, K., Israel, G., Falanga, M., Ramsay, G., Masetti, N., 2015. Swift J0525.6 + 2416 and IGR J04571 + 4527: two new hard X-ray-selected magnetic cataclysmic variables identified with XMM-Newton. MNRAS 453 (3), 3100–3106. https://doi.org/10.1093/mnras/stv1673.
Bernardini, F., de Martino, D., Mukai, K., Russell, D.M., Falanga, M., Masetti, N., Ferrigno, C., Israel, G., 2017. Broad-band characteristics of seven new hard X-ray selected cataclysmic variables. MNRAS 470 (4), 4815–4837. https://doi.org/10.1093/mnras/stx1494.
Bikmaev, I.F., Revnivtsev, M.G., Burenin, R.A., Sunyaev, R.A., 2006. XSS J00564 + 4548 and IGR J00234 + 6141: new cataclysmic variables from the RXTE and INTEGRAL all-sky surveys. Astron. Lett. 32 (9), 588–593. https://doi.org/10.1134/S1063773706090039.
Bird, A.J., Bazzano, A., Malizia, A., Fiocchi, M., Sguera, V., Bassani, L., Hill, A.B.,

Ubertini, P., Winkler, C., 2016. The IBIS soft gamma-Ray sky after 1000 integral orbits. ApJs 223 (1), 15. https://doi.org/10.3847/0067-0049/223/1/15.
Brunschweiger, J., Greiner, J., Ajello, M., Osborne, J., 2009. Intermediate polars in the Swift/BAT survey: spectra and white dwarf masses. A&A 496 (1), 121–127. https://doi.org/10.1051/0004-6361/200811285.
Brunschweiger, J., Greiner, J., Ajello, M., Osborne, J., 2009. Intermediate polars in the Swift/BAT survey: spectra and white dwarf masses. A&A 496 (1), 121–127. https://doi.org/10.1051/0004-6361/200811285.
Buckley, D.A.H., Sullivan, D.J., Remillard, R.A., Tuohy, I.R., Clark, M., 1990. LB 1800: a bright eclipsing cataclysmic variable and a transient X-Ray source. ApJ 355, 617. https://doi.org/10.1086/168794.
Burenin, R.A., Revnivtsev, M.G., Tkachenko, A.Y., Vorob'ev, V.S., Semena, A.N., Meshcheryakov, A.V., Dodonov, S.N., Eselevich, M.V., Pavlinsky, M.N., 2016. Sample of cataclysmic variables detected in the 400d X-ray survey. Astron. Lett. 42 (4), 240–250. https://doi.org/10.1134/S1063773716040022.
Butters, O.W., Norton, A.J., Hakala, P., Mukai, K., Barlow, E.J., 2008. RXTE Determination of the intermediate polar status of XSS J00564 + 4548, IGR J17195-4100, and XSS J12270-4859. A&A 487 (1), 271–276. https://doi.org/10.1051/0004-6361:200809942.
Butters, O.W., Norton, A.J., Mukai, K., Tomsick, J.A., 2011. RXTE and XMM observations of intermediate polar candidates. A&A 526, A77. https://doi.org/10.1051/0004-6361/201015848.
Byckling, K., Mukai, K., Thorstensen, J.R., Osborne, J.P., 2010. Deriving an X-ray luminosity function of dwarf novae based on parallax measurements. MNRAS 408 (4), 2298–2311. https://doi.org/10.1111/j.1365-2966.2010.17276.x.
Canalle, J.B.G., Saxton, C.J., Wu, K., Cropper, M., Ramsay, G., 2005. Accretion in dipole magnetic fields: flow structure and X-ray emission of accreting white dwarfs. A&A 440 (1), 185–198. https://doi.org/10.1051/0004-6361:20052706.
Charles, P., Thorstensen, J., Bowyer, S., Middleditch, J., 1979. 2A 0526-328: an X-ray-emitting cataclysmic variable. ApJL 231, L131–L135. https://doi.org/10.1086/183019.
Chernyakova, M., Courvoisier, T.J.-L., Rodriguez, J., Lutovinov, A., 2005. INTEGRAL discovery of the new source IGR J12349-6434. The Astronomer's Telegram 519, 1.
Clavel, M., Tomsick, J., Rahoui, F., Krivonos, R., 2016. Identifying IGR J18293-1213 and IGR J14091-6108 as magnetic CVs. 41st COSPAR Scientific Assembly. Vol. 41.
Clavel, M., Tomsick, J. A., Hare, J., Krivonos, R., Mori, K., Stern, D., 2019. NuSTAR observations of the unidentified INTEGRAL sources: constraints on the Galactic population of HMXBs. arXiv preprint: 1910.02855.
Collaboration, G., 2018. Gaia data release 2. Summary of the contents and survey properties. A&A 616, A1. https://doi.org/10.1051/0004-6361/201833051.
Cordova, F.A., Mason, K.O., Nelson, J.E., 1981. X-ray observations of selected cataclysimic variable stars using the Einstein observatory. ApJ 245, 609–617. https://doi.org/10.1086/158836.
Cropper, M., Ramsay, G., Wu, K., 1998. White dwarf masses in magnetic cataclysmic variables: multi-temperature FITS to GINGA data. MNRAS 293 (3), 222–232. https://doi.org/10.1046/j.1365-8711.1998.00610.x.
Cropper, M., Wu, K., Ramsay, G., Kocabiyik, A., 1999. Effects of gravity on the structure of post-shock accretion flows in magnetic cataclysmic variables. MNRAS 306 (3), 684–690. https://doi.org/10.1046/j.1365-8711.1999.02570.x.
Done, C., Osborne, J.P., 1997. The X-ray spectrum of the dwarf nova SS CYG in quiescence and outburst. MNRAS 288 (3), 649–664. https://doi.org/10.1093/mnras/288.3.649.
Ducci, L., Doroshenko, V., Suleimanov, V., Nikołajuk, M., Santangelo, A., Ferrigno, C., 2016. RT Crucis: a look into the X-ray emission of a peculiar symbiotic star. A&A 592, A58. https://doi.org/10.1051/0004-6361/201628242.
Evans, P.A., Beardmore, A.P., Osborne, J.P., 2008. Swift-XRT identification of IGR J19267 + 1325 as an intermediate polar. Astronomer's Telegram 1669, 1.
Eze, R.N.C., Luna, G.J.M., Smith, R.K., 2010. High-Resolution X-ray spectra of the symbiotic star SS73 17. ApJ 709 (2), 816–822. https://doi.org/10.1088/0004-637X/709/2/816.
Fabian, A.C., Pringle, J.E., Rees, M.J., 1976. X-ray emission from accretion on to white dwarfs. MNRAS 175, 43–60. https://doi.org/10.1093/mnras/175.1.43.
Falanga, M., Bonnet-Bidaud, J.M., Suleimanov, V., 2005. INTEGRAL broadband X-ray spectrum of the intermediate polar V709 Cassiopeiae. A&A 444 (2), 561–564. https://doi.org/10.1051/0004-6361:20054002.
Ferrario, L., de Martino, D., Gänsicke, B.T., 2015. Magnetic white dwarfs. Space Sci. Rev. 191 (1–4), 111–169. https://doi.org/10.1007/s11214-015-0152-0.
Fortin, F., Chaty, S., Coleiro, A., Tomsick, J.A., Nitschelm, C.H.R., 2018. Spectroscopic identification of INTEGRAL high-energy sources with VLT/ISAAC. A&A 618, A150. https://doi.org/10.1051/0004-6361/201731265.
Frank, J., King, A., Raine, D.J., 2002. Accretion power in astrophysics: third edition.
Gaensicke, B.T., Marsh, T.R., Edge, A., Rodriguez-Gil, P., Steeghs, D., Araujo-Betancor, S., Harlaftis, E., Giannakis, O., Pyrzas, S., Morales-Rueda, L., Aungwerojwit, A., 2005. IGR J17303-0601 is a new intermediate polar. Astronomer's Telegram 463, 1.
Gehrels, N., Chincarini, G., Giommi, P., Mason, K.O., Nousek, J.A., Wells, A.A., White, N.E., Barthelmy, S.D., Burrows, D.N., Cominsky, L.R., Hurley, K.C., Marshall, F.E., Mészáros, P., Roming, P.W.A., Angelini, L., Barbier, L.M., Belloni, T., Campana, S., Caraveo, P.A., Chester, M.M., Citterio, O., Cline, T.L., Cropper, M.S., Cummings, J.R., Dean, A.J., Feigelson, E.D., Fenimore, E.E., Frail, D.A., Fruchter, A.S., Garmire, G.P., Gendreau, K., Ghisellini, G., Greiner, J., Hill, J.E., Hunsberger, S.D., Krimm, H.A., Kulkarni, S.R., Kumar, P., Lebrun, F., Lloyd-Ronning, N.M., Markwardt, C.B., Mattson, B.J., Mushotzky, R.F., Norris, J.P., Osborne, J., Paczynski, B., Palmer, D.M., Park, H.-S., Parsons, A.M., Paul, J., Rees, M.J., Reynolds, C.S., Rhoads, J.E., Sasseen, T.P., Schaefer, B.E., Short, A.T., Smale, A.P., Smith, I.A., Stella, L., Tagliaferri, G., Takahashi, T., Tashiro, M., Townsley, L.K., Tueller, J., Turner, M.J.L., Vietri, M., Voges, W., Ward, M.J., Willingale, R., Zerbi, F.M., Zhang, W.W., 2004. The Swift gamma-ray burst mission. ApJ 611 (2), 1005–1020. https://doi.org/10.1086/422091.
Giacconi, R., Murray, S., Gursky, H., Kellogg, E., Schreier, E., Matilsky, T., Koch, D., Tananbaum, H., 1974. The third UHURU catalog of X-ray sources. ApJs 27, 37. https://doi.org/10.1086/190288.
Goliasch, J., Nelson, L., 2015. Population synthesis of cataclysmic variables. I. Inclusion of detailed nuclear evolution. ApJ 809 (1), 80. https://doi.org/10.1088/0004-637X/809/1/80.
Grebenev, S.A., Mereminskiy, I.A., 2015. JEM-X/INTEGRAL X-ray survey of the galactic center region. Astron. Lett. 41 (12), 765–784. https://doi.org/10.1134/S1063773715120038.
Griffiths, R.E., Lamb, D.Q., Ward, M.J., Wilson, A.S., Charles, P.A., Thorstensen, J., McHardy, I.M., Lawrence, A., 1980. The optical identification of H 2252-035 with a cataclysmic variable. MNRAS 193, 25P–33. https://doi.org/10.1093/mnras/193.1.25P.
Haberl, F., Israel, G.L., Rodriguez Castillo, G.A., Vasilopoulos, G., Delvaux, C., De Luca, A., Carpano, S., Esposito, P., Novara, G., Salvaterra, R., Tiengo, A., D'Agostino, D., Udalski, A., 2017. EXTraS discovery of two pulsators in the direction of the LMC: a Be/X-ray binary pulsar in the LMC and a candidate double-degenerate polar in the foreground. A&A 598, A69. https://doi.org/10.1051/0004-6361/201629744.
Hailey, C.J., Mori, K., Perez, K., Canipe, A.M., Hong, J., Tomsick, J.A., Boggs, S.E., Christensen, F.E., Craig, W.W., Fornasini, F., Grindlay, J.E., Harrison, F.A., Nynka, M., Rahoui, F., Stern, D., Zhang, S., Zhang, W.W., 2016. Evidence for intermediate polars as the origin of the galactic center hard X-ray emission. ApJ 826 (2), 160. https://doi.org/10.3847/0004-637X/826/2/160.
Halpern, J.P., Gotthelf, E.V., 2010. AX J1740.2-2903: optical period confirms intermediate polar classification. Astronomer's Telegram 2681, 1.
Halpern, J.P., Thorstensen, J.R., Cho, P., Collver, G., Motsoaledi, M., Breytenbach, H., Buckley, D.A.H., Woudt, P.A., 2018. Optical studies of 15 hard X-ray selected cataclysmic binaries. AJ 155 (6), 247. https://doi.org/10.3847/1538-3881/aabfd0.
Heise, J., Mewe, R., Brinkman, A.C., Gronenschild, E.H.B.M., den Boggende, A.J.F., Schrijver, J., Parsignault, D.R., Grindlay, J.E., 1978. Detection of both soft and hard X-ray emission from SS Cygni with ANS. A&A 63, L1–L3.
Hernanz, M., 2014. V2487 Oph 1998: a post nova in an intermediate polar. European Physical Journal Web of Conferences. European Physical Journal Web of Conferences Vol. 64. pp. 07002. https://doi.org/10.1051/epjconf/20136407002.
Hong, J., Mori, K., Hailey, C.J., Nynka, M., Zhang, S., Gotthelf, E., Fornasini, F.M., Krivonos, R., Bauer, F., Perez, K., Tomsick, J.A., Bodaghee, A., Chiu, J.-L., Clavel, M., Stern, D., Grindlay, J.E., Alexander, D.M., Aramaki, T., Baganoff, F.K., Barret, D., Barrière, N., Boggs, S.E., Canipe, A.M., Christensen, F.E., Craig, W.W., Desai, M.A., Forster, K., Giommi, P., Grefenstette, B.W., Harrison, F.A., Hong, D., Hornstrup, A., Kitaguchi, T., Koglin, J.E., Madsen, K.K., Mao, P.H., Miyasaka, H., Perri, M., Pivovaroff, M.J., Puccetti, S., Rana, V., Westergaard, N.J., Zhang, W.W., Zoglauer, A., 2016. NuSTAR hard X-ray survey of the galactic center region. II. X-ray point sources. ApJ 825 (2), 132. https://doi.org/10.3847/0004-637X/825/2/132.
Ishida, M., 1991. -.
Johnson, C.B., Torres, M.A.P., Hynes, R.I., Jonker, P.G., Heinke, C., Maccarone, T., Britt, C.T., Steeghs, D., Wevers, T., Wu, J., 2017. CXOGBS J174954.5-294335: a new deeply eclipsing intermediate polar. MNRAS 466 (1), 129–137. https://doi.org/10.1093/mnras/stw3063.
Karasev, D.I., Lutovinov, A.A., Revnivtsev, M.G., Krivonos, R.A., 2012. Accurate localization and identification of six hard X-ray sources from Chandra and XMM-Newton data. Astron. Lett. 38 (10), 629–637. https://doi.org/10.1134/S1063773712100039.
Karasev, D.I., Tsygankov, S.S., Lutovinov, A.A., 2015. IGR J17463-2854, a possible symbiotic binary system in the galactic center region. Astron. Lett. 41 (8), 394–406. https://doi.org/10.1134/S1063773715080022.
Koyama, K., Makishima, K., Tanaka, Y., Tsunemi, H., 1986. Thermal X-ray emission with intense 6.7-kev iron line from the galactic ridge. PASJ 38, 121–131.
Krivonos, R., Revnivtsev, M., Churazov, E., Sazonov, S., Grebenev, S., Sunyaev, R., 2007. Hard X-ray emission from the Galactic ridge. A&A 463 (3), 957–967. https://doi.org/10.1051/0004-6361:20065626.
Krivonos, R., Revnivtsev, M., Lutovinov, A., Sazonov, S., Churazov, E., Sunyaev, R., 2007. INTEGRAL/IBIS all-sky survey in hard X-rays. A&A 475 (2), 775–784. https://doi.org/10.1051/0004-6361:20077191.
Krivonos, R., Tsygankov, S., Lutovinov, A., Revnivtsev, M., Churazov, E., Sunyaev, R., 2012. INTEGRAL/IBIS nine-year Galactic hard X-ray survey. A&A 545, A27. https://doi.org/10.1051/0004-6361/201219617.
Krivonos, R.A., Tsygankov, S.S., Mereminskiy, I.A., Lutovinov, A.A., Sazonov, S.Y., Sunyaev, R.A., 2017. New hard X-ray sources discovered in the ongoing INTEGRAL galactic plane survey after 14 yr of observations. MNRAS 470 (1), 512–516. https://doi.org/10.1093/mnras/stx1276.
Lamb, D.Q., Masters, A.R., 1979. X and UV radiation from accreting magnetic degenerate dwarfs. ApJL 234, L117–L122. https://doi.org/10.1086/183121.
Landi, R., Bassani, L., Dean, A.J., Bird, A.J., Fiocchi, M., Bazzano, A., Nousek, J.A., Osborne, J.P., 2009. INTEGRAL/IBIS and Swift/XRT observations of hard cataclysmic variables. MNRAS 392 (2), 630–640. https://doi.org/10.1111/j.1365-2966.2008.14086.x.
Lebrun, F., Leray, J.P., Lavocat, P., Crétolle, J., Arquès, M., Blondel, C., Bonnin, C., Bouère, A., Cara, C., Chaleil, T., Daly, F., Desages, F., Dzitko, H., Horeau, B., Laurent, P., Limousin, O., Mathy, F., Mauguen, V., Meignier, F., Molinié, F., Poindron, E., Rouger, M., Sauvageon, A., Tourrette, T., 2003. ISGRI: The INTEGRAL soft gamma-Ray imager. A&A 411, L141–L148. https://doi.org/10.1051/0004-6361:20031367.
Lebrun, F., Terrier, R., Bazzano, A., Bélanger, G., Bird, A., Bouchet, L., Dean, A., Del Santo, M., Goldwurm, A., Lund, N., Morand, H., Parmar, A., Paul, J., Roques, J.-P., Schönfelder, V., Strong, A.W., Ubertini, P., Walter, R., Winkler, C., 2004. Compact sources as the origin of the soft γ-ray emission of the Milky Way. Nature 428 (6980),

293–296. https://doi.org/10.1038/nature02407.
Lewin, W.H.G., Ricker, G.R., McClintock, J.E., 1971. X-rays from a new variable source GX 1 + 4. ApJ 169, L17. https://doi.org/10.1086/180805.
Luna, G.J.M., Mukai, K., Sokoloski, J.L., Lucy, A.B., Cusumano, G., Segreto, A., Jaque Arancibia, M., Nuñez, N.E., Puebla, R.E., Nelson, T., Walter, F., 2018. X-Ray, UV, and optical observations of the accretion disk and boundary layer in the symbiotic star RT Crucis. A&A 616, A53. https://doi.org/10.1051/0004-6361/201832592.
Luna, G.J.M., Raymond, J.C., Brickhouse, N.S., Mauche, C.W., Suleimanov, V., 2015. Testing the cooling flow model in the intermediate polar EX Hydrae. A&A 578, A15. https://doi.org/10.1051/0004-6361/201525755.
Luna, G.J.M., Sokoloski, J.L., 2007. The nature of the hard X-Ray-Emitting symbiotic star RT Cru. ApJ 671 (1), 741–747. https://doi.org/10.1086/522576.
Luna, G.J.M., Sokoloski, J.L., Mukai, K., Nelson, T., 2013. Symbiotic stars in X-rays. A&A 559, A6. https://doi.org/10.1051/0004-6361/201220792.
Lutovinov, A.A., Burenin, R.A., Revnivtsev, M.G., Bikmaev, I.F., 2012. Optical identification of six hard X-ray sources from the INTEGRAL and SWIFT all-sky surveys. Astron. Lett. 38 (1), 1–11. https://doi.org/10.1134/S1063773712010045.
Lutovinov, A.A., Burenin, R.A., Revnivtsev, M.G., Suleimanov, V.F., Tkachenko, A.Y., 2010. IGR J16547-1916/1RXS J165443.5-191620—a new intermediate polar from the INTEGRAL galactic survey. Astron. Lett. 36 (12), 904–909. https://doi.org/10.1134/S1063773710120042.
Marcu, D.M., Fürst, F., Pottschmidt, K., Grinberg, V., Müller, S., Wilms, J., Postnov, K.A., Corbet, R.H.D., Markwardt, C.B., Cadolle Bel, M., 2011. The 5 hr pulse period and broadband spectrum of the symbiotic X-Ray binary 3A 1954 + 319. ApJL 742 (1), L11. https://doi.org/10.1088/2041-8205/742/1/L11.
de Martino, D., Bernardini, F., Mukai, K., Falanga, M., Masetti, N., 2019. Hard X-ray Cataclysmic Variables. arXiv preprint: 1909.0630610.1016/j.asr.2019.09.006.
de Martino, D., Falanga, M., Bonnet-Bidaud, J.-M., Belloni, T., Mouchet, M., Masetti, N., Andruchow, I., Cellone, S.A., Mukai, K., Matt, G., 2010. The intriguing nature of the high-energy gamma ray source XSS J12270-4859. A&A 515, A25. https://doi.org/10.1051/0004-6361/200913802.
de Martino, D., Matt, G., Mukai, K., Bonnet-Bidaud, J.-M., Falanga, M., Gänsicke, B.T., Haberl, F., Marsh, T.R., Mouchet, M., Littlefair, S.P., Dhillon, V., 2008. 1RXS J173021.5-055933: a cataclysmic variable with a fast-spinning magnetic white dwarf. A&A 481 (1), 149–159. https://doi.org/10.1051/0004-6361:20078368.
Masetti, N., Bassani, L., Dean, A.J., Ubertini, P., Walter, R., 2006. The symbiotic star CD-57 3057 is the likely counterpart of IGR J10109-5746. Astronomer's Telegram 715, 1.
Masetti, N., Mason, E., Morelli, L., Cellone, S.A., McBride, V.A., Palazzi, E., Bassani, L., Bazzano, A., Bird, A.J., Charles, P.A., Dean, A.J., Galaz, G., Gehrels, N., Landi, R., Malizia, A., Minniti, D., Panessa, F., Romero, G.E., Stephen, J.B., Ubertini, P., Walter, R., 2008. Unveiling the nature of INTEGRAL objects through optical spectroscopy. VI. A multi-observatory identification campaign. A&A 482 (1), 113–132. https://doi.org/10.1051/0004-6361:20079332.
Masetti, N., Morelli, L., Palazzi, E., Galaz, G., Bassani, L., Bazzano, A., Bird, A.J., Dean, A.J., Israel, G.L., Landi, R., Malizia, A., Minniti, D., Schiavone, F., Stephen, J.B., Ubertini, P., Walter, R., 2006. Unveiling the nature of INTEGRAL objects through optical spectroscopy. V. Identification and properties of 21 southern hard X-ray sources. A&A 459 (1), 21–30. https://doi.org/10.1051/0004-6361:20066055.
Masetti, N., Parisi, P., Palazzi, E., Jiménez-Bailón, E., Chavushyan, V., Bassani, L., Bazzano, A., Bird, A.J., Dean, A.J., Charles, P.A., Galaz, G., Landi, R., Malizia, A., Mason, E., McBride, V.A., Minniti, D., Morelli, L., Schiavone, F., Stephen, J.B., Ubertini, P., 2010. Unveiling the nature of INTEGRAL objects through optical spectroscopy. VIII. Identification of 44 newly detected hard X-ray sources. A&A 519, A96. https://doi.org/10.1051/0004-6361/201014852.
Masetti, N., Parisi, P., Palazzi, E., Jiménez-Bailón, E., Chavushyan, V., McBride, V., Rojas, A.F., Steward, L., Bassani, L., Bazzano, A., Bird, A.J., Charles, P.A., Galaz, G., Landi, R., Malizia, A., Mason, E., Minniti, D., Morelli, L., Schiavone, F., Stephen, J.B., Ubertini, P., 2013. Unveiling the nature of INTEGRAL objects through optical spectroscopy. X. A new multi-year, multi-observatory campaign. A&A 556, A120. https://doi.org/10.1051/0004-6361/201322026.
Masetti, N., Parisi, P., Palazzi, E., Jiménez-Bailón, E., Morelli, L., Chavushyan, V., Mason, E., McBride, V.A., Bassani, L., Bazzano, A., Bird, A.J., Dean, A.J., Galaz, G., Gehrels, N., Landi, R., Malizia, A., Minniti, D., Schiavone, F., Stephen, J.B., Ubertini, P., 2009. Unveiling the nature of INTEGRAL objects through optical spectroscopy. VII. Identification of 20 Galactic and extragalactic hard X-ray sources. A&A 495 (1), 121–135. https://doi.org/10.1051/0004-6361:200811322.
Merloni, A., Predehl, P., Becker, W., Böhringer, H., Boller, T., Brunner, H., Brusa, M., Dennerl, K., Freyberg, M., Friedrich, P., Georgakakis, A., Haberl, F., Hasinger, G., Meidinger, N., Mohr, J., Nandra, K., Rau, A., Reiprich, T. H., Robrade, J., Salvato, M., Santangelo, A., Sasaki, M., Schwope, A., Wilms, J., German eROSITA Consortium, t., 2012. eROSITA Science Book: Mapping the Structure of the Energetic Universe. arXiv preprint: 1209.3114.
McGowan, K.E., Priedhorsky, W.C., Trudolyubov, S.P., 2004. On the correlated X-ray and optical evolution of SS Cygni. ApJ 601 (2), 1100–1108. https://doi.org/10.1086/380758.
Middleton, M.J., Cackett, E.M., Shaw, C., Ramsay, G., Roberts, T.P., Wheatley, P.J., 2012. Identifying a new intermediate polar using XMM-Newton and INTEGRAL. MNRAS 419 (1), 336–341. https://doi.org/10.1111/j.1365-2966.2011.19696.x.
Muerset, U., Wolff, B., Jordan, S., 1997. X-ray properties of symbiotic stars. II. Systems with colliding winds. A&A 319, 201–210.
Mukai, K., 2017. X-Ray emissions from accreting white dwarfs: a review. PASP 129 (976), 062001. https://doi.org/10.1088/1538-3873/aa6736.
Mukai, K., Rana, V., Bernardini, F., de Martino, D., 2015. Unambiguous detection of reflection in magnetic cataclysmic variables: joint NuSTAR-XMM-Newton observations of three intermediate polars. ApJL 807 (2), L30. https://doi.org/10.1088/2041-8205/807/2/L30.
Mukai, K., Shiokawa, K., 1993. The EXOSAT medium energy (ME) sample of dwarf novae. ApJ 418, 863. https://doi.org/10.1086/173444.
Munari, U., 2019. The Symbiotic Stars. arXiv preprint: 1909.01389.
Munari, U., Dallaporta, S., Cherini, G., 2016. The 2015 super-active state of recurrent nova T CrB and the long term evolution after the 1946 outburst. New Astron. 47, 7–15. https://doi.org/10.1016/j.newast.2016.01.002.
Narayan, R., Popham, R., 1993. Hard X-rays from accretion disk boundary layers. Nature 362 (6423), 820–822. https://doi.org/10.1038/362820a0.
Nauenberg, M., 1972. Analytic approximations to the mass-radius relation and energy of zero-temperature stars. ApJ 175, 417. https://doi.org/10.1086/151568.
Nespoli, E., Fabregat, J., Mennickent, R.E., 2008. IGR J16358-4726 and IGR J16393-4643: two new symbiotic X-ray binaries. Astronomer's Telegram 1450, 1.
Nichelli, E., Israel, G.L., Moretti, A., Campana, S., Bernabei, S., Mason, E., Götz, D., Stella, L., 2009. Swift-XRT detection of x-ray pulsations from IGR J18173-2509 and SWIFT J2138.8 + 5544. Astronomer's Telegram 2354, 1.
Norton, A.J., Beardmore, A.P., Retter, A., Buckley, D.A.H., 2000. The nature of TW Pictoris. MNRAS 312 (2), 362–370. https://doi.org/10.1046/j.1365-8711.2000.03216.x.
Norton, A.J., Wynn, G.A., Somerscales, R.V., 2004. The spin periods and magnetic moments of white dwarfs in magnetic cataclysmic variables. ApJ 614 (1), 349–357. https://doi.org/10.1086/423333.
Ottmann, R., Schmitt, J.H.M.M., 1992. The contributions of RS CVn systems to the diffuse X-ray background. A&A 256, 421–427.
Pala, A. F., Gänsicke, B. T., Breedt, E., Knigge, C., Hermes, J. J., Gentile Fusillo, N. P., Hollands, M. A., Naylor, T., Pelisoli, I., Toonen, S., Aungwerojwit, A., Cukanovaite, E., Dennihy, E., Manser, C. J., Pretorius, M. L., Scaringi, S., Schreiber, M. R., Toloza, O., 2019. The space density of cataclysmic variables from *Gaia* DR2. arXiv preprint: 1907.13152.
Valinia, A., Marshall, F.E., 1998. RXTE measurement of the diffuse X-ray emission from the galactic ridge: implications for the energetics of the interstellar medium. ApJ 505 (1), 134–147. https://doi.org/10.1086/306155.
van Paradijs, J., Verbunt, F., 1984. A comparison of soft x-ray transients and dwarf novae. In: Woosley, S.E. (Ed.), American Institute of Physics Conference Series. Vol. 115. pp. 49–62. https://doi.org/10.1063/1.34556.
Patterson, J., 1984. The evolution of cataclysmic and low-mass X-ray binaries. ApJs 54, 443–493. https://doi.org/10.1086/190940.
Patterson, J., Raymond, J.C., 1985. X-Ray emission from cataclysmic variables with accretion disks. I. Hard X-rays. ApJ 292, 535–549. https://doi.org/10.1086/163187.
Pavlinsky, M., Levin, V., Akimov, V., Krivchenko, A., Rotin, A., Kuznetsova, M., Lapshov, I., Tkachenko, A., Krivonos, R., Semena, N., Buntov, M., Glushenko, A., Arefiev, V., Yaskovich, A., Grebenev, S., Sazonov, S., Lutovinov, A., Molkov, S., Serbinov, D., Kudelin, M., Drozdova, T., Voronkov, S., Sunyaev, R., Churazov, E., Gilfanov, M., Ramsey, B., O'Dell, S.L., Kolodziejczak, J., Zavlin, V., Swartz, D., 2018. ART-XC / SRG overview. Proc. SPIE. Society of Photo-Optical Instrumentation Engineers (SPIE) Conference Series Vol. 10699. pp. 106991Y. https://doi.org/10.1117/12.2312053.
Perez, K., Hailey, C.J., Bauer, F.E., Krivonos, R.A., Mori, K., Baganoff, F.K., Barrière, N.M., Boggs, S.E., Christensen, F.E., Craig, W.W., Grefenstette, B.W., Grindlay, J.E., Harrison, F.A., Hong, J., Madsen, K.K., Nynka, M., Stern, D., Tomsick, J.A., Wik, D.R., Zhang, S., Zhang, W.W., Zoglauer, A., 2015. Extended hard-X-ray emission in the inner few parsecs of the Galaxy. Nature 520 (7549), 646–649. https://doi.org/10.1038/nature14353.
Popham, R., Narayan, R., 1995. Accretion disk boundary layers in cataclysmic variables. I. Optically thick boundary layers. ApJ 442, 337. https://doi.org/10.1086/175444.
Pretorius, M.L., Knigge, C., 2012. The space density and X-ray luminosity function of non-magnetic cataclysmic variables. MNRAS 419 (2), 1442–1454. https://doi.org/10.1111/j.1365-2966.2011.19801.x.
Pretorius, M.L., Knigge, C., Schwope, A.D., 2013. The space density of magnetic cataclysmic variables. MNRAS 432 (1), 570–583. https://doi.org/10.1093/mnras/stt499.
Pretorius, M.L., Mukai, K., 2014. Constraints on the space density of intermediate polars from the Swift-BAT survey. MNRAS 442 (3), 2580–2585. https://doi.org/10.1093/mnras/stu990.
Pringle, J.E., Savonije, G.J., 1979. X-Ray emission from dwarf novae. MNRAS 187, 777–783. https://doi.org/10.1093/mnras/187.4.777.
Rahoui, F., Tomsick, J.A., Krivonos, R., 2017. Identifying four INTEGRAL sources in the Galactic plane via VLT/optical and XMM-Newton/X-ray spectroscopy. MNRAS 465 (2), 1563–1572. https://doi.org/10.1093/mnras/stw2830.
Rahoui, F., Tomsick, J.A., Krivonos, R., 2017. Identifying four INTEGRAL sources in the Galactic plane via VLT/optical and XMM-Newton/X-ray spectroscopy. MNRAS 465 (2), 1563–1572. https://doi.org/10.1093/mnras/stw2830.
Ramsay, G., 2000. Determining the mass of the accreting white dwarf in magnetic cataclysmic variables using RXTE data. MNRAS 314 (2), 403–408. https://doi.org/10.1046/j.1365-8711.2000.03239.x.
Revnivtsev, M.G., Lutovinov, A.A., Suleimanov, B.F., Molkov, S.V., Sunyaev, R.A., 2004. Broadband X-ray spectrum of the intermediate polar V2400 Oph. Astron. Lett. 30 (11), 772–778. https://doi.org/10.1134/1.1819495.
Revnivtsev, M., Lutovinov, A., Suleimanov, V., Sunyaev, R., Zheleznyakov, V., 2004. Broadband X-ray spectrum of intermediate polar V1223 Sgr. A&A 426, 253–256. https://doi.org/10.1051/0004-6361:20040498.
Revnivtsev, M., Sazonov, S., Churazov, E., Forman, W., Vikhlinin, A., Sunyaev, R., 2009. Discrete sources as the origin of the Galactic X-ray ridge emission. Nature 458 (7242), 1142–1144. https://doi.org/10.1038/nature07946.
Revnivtsev, M., Sazonov, S., Forman, W., Churazov, E., Sunyaev, R., 2011. Luminosity function of faint Galactic sources in the Chandra bulge field. MNRAS 414 (1), 495–499. https://doi.org/10.1111/j.1365-2966.2011.18411.x.
Revnivtsev, M., Sazonov, S., Gilfanov, M., Churazov, E., Sunyaev, R., 2006. Origin of the Galactic ridge X-ray emission. A&A 452 (1), 169–178. https://doi.org/10.1051/

0004-6361:20054268.
Revnivtsev, M., Sazonov, S., Jahoda, K., Gilfanov, M., 2004. RXTE all-sky slew survey. Catalog of X-ray sources at b > 10°. A&A 418, 927–936. https://doi.org/10.1051/0004-6361:20035798.
Revnivtsev, M., Sazonov, S., Krivonos, R., Ritter, H., Sunyaev, R., 2008. Properties of the Galactic population of cataclysmic variables in hard X-rays. A&A 489 (3), 1121–1127. https://doi.org/10.1051/0004-6361:200810213.
Revnivtsev, M., Sazonov, S., Sunyaev, R., 2007. Origin of the Galactic Ridge X-ray Emission. Progr. Theor. Phys. Suppl. 169, 125–130. https://doi.org/10.1143/PTPS.169.125.
Revnivtsev, M.G., Kniazev, A.Y., Sazonov, S.Y., Burenin, R.A., Tekola, A., Buckley, D.A.H., Pretorius, M.L., Menzies, J., Lawson, W., 2009. Optical identification of the source IGR J08390-4833 from the INTEGRAL all-sky survey. Astron. Lett. 35 (1), 33–38. https://doi.org/10.1134/S1063773709010046.
Revnivtsev, M.G., Sazonov, S.Y., Molkov, S.V., Lutovinov, A.A., Churazov, E.M., Sunyaev, R.A., 2006. Hard X-ray survey of the Galactic plane region in Crux: a catalog of sources. Astron. Lett. 32 (3), 145–148. https://doi.org/10.1134/S1063773706030017.
Ritter, H., Kolb, U., 2003. Catalogue of cataclysmic binaries, low-mass X-ray binaries and related objects (seventh edition). A&A 404, 301–303. https://doi.org/10.1051/0004-6361:20030330.
Rodriguez, J., Tomsick, J.A., Chaty, S., 2009. Swift follow-up observations of 17 INTEGRAL sources of uncertain or unknown nature. A&A 494, 417–428. https://doi.org/10.1051/0004-6361:200810773.
Rothschild, R.E., Gruber, D.E., Knight, F.K., Matteson, J.L., Nolan, P.L., Swank, J.H., Holt, S.S., Serlemitsos, P.J., Mason, K.O., Tuohy, I.R., 1981. The X-ray sxpectrum of AM HER from 0.1 to 150 KEV. ApJ 250, 723–732. https://doi.org/10.1086/159420.
Saxton, C.J., Wu, K., Canalle, J.a.B.G., Cropper, M., Ramsay, G., 2007. X-ray emissions from two-temperature accretion flows within a dipole magnetic funnel. MNRAS 379 (2), 779–790. https://doi.org/10.1111/j.1365-2966.2007.11958.x.
Sazonov, S., Revnivtsev, M., Gilfanov, M., Churazov, E., Sunyaev, R., 2006. X-ray luminosity function of faint point sources in the Milky Way. A&A 450 (1), 117–128. https://doi.org/10.1051/0004-6361:20054297.
Schwope, A.D., 2018. Exploring the space density of X-ray selected cataclysmic variables. A&A 619, A62. https://doi.org/10.1051/0004-6361/201833723.
Schwope, A.D., Brunner, H., Buckley, D., Greiner, J., Heyden, K.v.d., Neizvestny, S., Potter, S., Schwarz, R., 2002. The census of cataclysmic variables in the ROSAT bright survey. A&A 396, 895–910. https://doi.org/10.1051/0004-6361:20021386.
Sguera, V., Bird, A.J., Sidoli, L., 2015. The symbiotic star RT Cru entered a new hard X-ray state as detected by INTEGRAL. Astronomer's Telegram 8448, 1.
Sguera, V., Drave, S.P., Sidoli, L., Fiocchi, M., Sokoloski, J.L., Bird, A.J., Bazzano, A., Bassani, L., Kuulkers, E., Malizia, A., Natalucci, L., Tarana, A., 2012. INTEGRAL detection of the symbiotic star RT Cru during a bright hard X-ray state. Astronomer's Telegram 3887, 1.
Shaw, A.W., Heinke, C.O., Mukai, K., Sivakoff, G.R., Tomsick, J.A., Rana, V., 2018. Measuring the masses of intermediate polars with NuSTAR: V709 Cas, NY Lup, and V1223 Sgr. MNRAS 476 (1), 554–561. https://doi.org/10.1093/mnras/sty246.
Skibo, J.G., Johnson, W.N., Kurfess, J.D., Kinzer, R.L., Jung, G., Grove, J.E., Purcell, W.R., Ulmer, M.P., Gehrels, N., Tueller, J., 1997. OSSE Observations of the soft gamma-Ray continuum from the galactic plane at longitude 95 degrees. ApJL 483 (2), L95–L98. https://doi.org/10.1086/310755.
Smith, R.K., Mushotzky, R., Mukai, K., Kallman, T., Markwardt, C.B., Tueller, J., 2008. The symbiotic system SS73 17 seen with Suzaku. PASJ 60, S43. https://doi.org/10.1093/pasj/60.sp1.S43.
Suleimanov, V., Hertfelder, M., Werner, K., Kley, W., 2014. Modeling the EUV spectra of optically thick boundary layers of dwarf novae in outburst. A&A 571, A55. https://doi.org/10.1051/0004-6361/201423724.
Suleimanov, V., Revnivtsev, M., Ritter, H., 2005. RXTE Broadband X-ray spectra of intermediate polars and white dwarf mass estimates. A&A 435 (1), 191–199. https://doi.org/10.1051/0004-6361:20041283.
Suleimanov, V., Doroshenko, V., Ducci, L., Zhukov, G.V., Werner, K., 2016. GK Persei and EX Hydrae: intermediate polars with small magnetospheres. A&A 591, A35. https://doi.org/10.1051/0004-6361/201628301.
Suleimanov, V.F., Doroshenko, V., Werner, K., 2019. Hard X-ray view on intermediate polars in the gaia era. MNRAS 482, 3622–3635. https://doi.org/10.1093/mnras/sty2952.
Swank, J.H., Boldt, E.A., Holt, S.S., Rothschild, R.E., Serlemitsos, P.J., 1978. Hard X-rays form U Geminorum. ApJL 226, L133–L136. https://doi.org/10.1086/182848.
Tanaka, Y., 2002. ASCA Observation of X-ray emission from the galactic ridge. A&A 382, 1052–1060. https://doi.org/10.1051/0004-6361:20011678.
Tapia, S., 1977. Discovery of a magnetic compact star in the AM Herculis / 3U 1809+50 system. ApJL 212, L125–L129. https://doi.org/10.1086/182390.
Terrier, R., Lebrun, F., Bélanger, G., Goldwurm, A., Strong, A.W., Schoenfelder, V., Bouchet, L., Roques, J.P., Parmar, A., 2004. Contribution of Point Sources to the Soft Gamma-Ray Galactic Emission. In: Schoenfelder, V., Lichti, G., Winkler, C. (Eds.), 5th INTEGRAL Workshop on the INTEGRAL Universe. ESA Special Publication Vol. 552. pp. 513.
Thorstensen, J.R., Halpern, J., 2013. Optical and X-ray studies of 10 X-ray-selected cataclysmic binaries. AJ 146 (5), 107. https://doi.org/10.1088/0004-6256/146/5/107.
Tomsick, J.A., Bodaghee, A., Chaty, S., Rodriguez, J., Rahoui, F., Halpern, J., Kalemci, E., Özbey Arabaci, M., 2012. Localizing INTEGRAL sources with Chandra: X-ray and multi-wavelength identifications and energy spectra. ApJ 754 (2), 145. https://doi.org/10.1088/0004-637X/754/2/145.
Tomsick, J.A., Chaty, S., Rodriguez, J., Walter, R., Kaaret, P., 2009. Chandra localizations and spectra of INTEGRAL sources in the galactic plane: the cycle 9 sample. ApJ 701 (1), 811–823. https://doi.org/10.1088/0004-637X/701/1/811.
Tomsick, J.A., Krivonos, R., Wang, Q., Bodaghee, A., Chaty, S., Rahoui, F., Rodriguez, J., Fornasini, F.M., 2016. Chandra observations of eight sources discovered by INTEGRAL. ApJ 816 (1), 38. https://doi.org/10.3847/0004-637X/816/1/38.
Tomsick, J.A., Rahoui, F., Krivonos, R., Clavel, M., Strader, J., Chomiuk, L., 2016. Identifying IGR J14091-6108 as a magnetic CV with a massive white dwarf using X-ray and optical observations. MNRAS 460 (1), 513–523. https://doi.org/10.1093/mnras/stw871.
Tovmassian, G., González-Buitrago, D., Thorstensen, J., Kotze, E., Breytenbach, H., Schwope, A., Bernardini, F., Zharikov, S.V., Hernandez, M.S., Buckley, D.A.H., de Miguel, E., Hambsch, F.-J., Myers, G., Goff, W., Cejudo, D., Starkey, D., Campbell, T., Ulowetz, J., Stein, W., Nelson, P., Reichart, D.E., Haislip, J.B., Ivarsen, K.M., LaCluyze, A.P., Moore, J.P., Miroshnichenko, A.S., 2017. IGR J19552+0044: A new asynchronous short period polar. filling the gap between intermediate and ordinary polars. A&A 608, A36. https://doi.org/10.1051/0004-6361/201731323.
Tovmassian, G., Szkody, P., Yarza, R., Kennedy, M., 2018. K2 Study of the magnetic precataclysmic variable V1082 Sagittarius. ApJ 863 (1), 47. https://doi.org/10.3847/1538-4357/aad229.
Tylenda, R., 1981. Viscous boundary layer and hard X-rays from dwarf novae. Acta Astronomica 31, 267–281.
Wada, Y., Yuasa, T., Nakazawa, K., Makishima, K., Hayashi, T., Ishida, M., 2018. An estimation of the white dwarf mass in the dwarf nova GK Persei with NuSTAR observations of two states. MNRAS 474 (2), 1564–1571. https://doi.org/10.1093/mnras/stx2880.
Warner, B., 2003. Cataclysmic variable stars. https://doi.org/10.1017/CBO9780511586491.
Warwick, R.S., Turner, M.J.L., Watson, M.G., Willingale, R., 1985. The galactic ridge observed by Exosat. Nature 317 (6034), 218–221. https://doi.org/10.1038/317218a0.
Winkler, C., Courvoisier, T.J.-L., Di Cocco, G., Gehrels, N., Giménez, A., Grebenev, S., Hermsen, W., Mas-Hesse, J.M., Lebrun, F., Lund, N., 2003. The INTEGRAL mission. A&A 411, L1–L6. https://doi.org/10.1051/0004-6361:20031288.
Woelk, U., Beuermann, K., 1996. Stationary radiation hydrodynamics of accreting magnetic white dwarfs. A&A 306, 232.
Worrall, D.M., Marshall, F.E., 1983. Stellar contributions to the hard X-ray galactic ridge. ApJ 267, 691–697. https://doi.org/10.1086/160906.
Worrall, D.M., Marshall, F.E., Boldt, E.A., Swank, J.H., 1982. HEAO-1 measurements of the galactic ridge. ApJ 255, 111–121. https://doi.org/10.1086/159809.
Wu, K., Chanmugam, G., Shaviv, G., 1994. Structure of steady state accretion shocks with several cooling functions: closed integral-form solution. ApJ 426, 664. https://doi.org/10.1086/174103.
Yuasa, T., Makishima, K., Nakazawa, K., 2012. Broadband spectral analysis of the galactic ridge X-Ray emission. ApJ 753 (2), 129. https://doi.org/10.1088/0004-637X/753/2/129.
Yuasa, T., Nakazawa, K., Makishima, K., Saitou, K., Ishida, M., Ebisawa, K., Mori, H., Yamada, S., 2010. White dwarf masses in intermediate polars observed with the Suzaku satellite. A&A 520, A25. https://doi.org/10.1051/0004-6361/201014542.
Zorotovic, M., Schreiber, M.R., Gänsicke, B.T., 2011. Post common envelope binaries from SDSS. XI. the white dwarf mass distributions of CVs and pre-CVs. A&A 536, A42. https://doi.org/10.1051/0004-6361/201116626.

Alexander Lutovinov is a specialist in the field of high-energy astrophysics and relativistic compact objects, author of more than 220 scientific publications, two monographs. He obtained PhD and Doctor degrees from Space Research Institute of RAS in 2000 and 2013, respectively. In 2013, he was awarded the Bredikhin Prize by Russian Academy of Sciences for outstanding achievements in astronomy. In 2015, Alexander Lutovinov was elected professor of the Russian Academy of Sciences. Currently he holds the position of the Deputy Director of the Space Research Institute of RAS.